

# Development of Energy Production Systems from Heat Produced in Deuterated Metals

Volume 2



**WARNING:**  
Please read the Export Control  
Agreement on the back cover.

*Technical Report*

---



# **Development of Energy Production Systems from Heat Produced in Deuterated Metals: Volume 2**

**TR-107843-V2**

Final Report, November 1999

EPRI Project Managers  
A. Machiels  
T. O. Passell

## **DISCLAIMER OF WARRANTIES AND LIMITATION OF LIABILITIES**

THIS DOCUMENT WAS PREPARED BY THE ORGANIZATION(S) NAMED BELOW AS AN ACCOUNT OF WORK SPONSORED OR COSPONSORED BY THE ELECTRIC POWER RESEARCH INSTITUTE, INC. (EPRI). NEITHER EPRI, ANY MEMBER OF EPRI, ANY COSPONSOR, THE ORGANIZATION(S) BELOW, NOR ANY PERSON ACTING ON BEHALF OF ANY OF THEM:

(A) MAKES ANY WARRANTY OR REPRESENTATION WHATSOEVER, EXPRESS OR IMPLIED, (I) WITH RESPECT TO THE USE OF ANY INFORMATION, APPARATUS, METHOD, PROCESS, OR SIMILAR ITEM DISCLOSED IN THIS DOCUMENT, INCLUDING MERCHANTABILITY AND FITNESS FOR A PARTICULAR PURPOSE, OR (II) THAT SUCH USE DOES NOT INFRINGE ON OR INTERFERE WITH PRIVATELY OWNED RIGHTS, INCLUDING ANY PARTY'S INTELLECTUAL PROPERTY, OR (III) THAT THIS DOCUMENT IS SUITABLE TO ANY PARTICULAR USER'S CIRCUMSTANCE; OR

(B) ASSUMES RESPONSIBILITY FOR ANY DAMAGES OR OTHER LIABILITY WHATSOEVER (INCLUDING ANY CONSEQUENTIAL DAMAGES, EVEN IF EPRI OR ANY EPRI REPRESENTATIVE HAS BEEN ADVISED OF THE POSSIBILITY OF SUCH DAMAGES) RESULTING FROM YOUR SELECTION OR USE OF THIS DOCUMENT OR ANY INFORMATION, APPARATUS, METHOD, PROCESS, OR SIMILAR ITEM DISCLOSED IN THIS DOCUMENT.

ORGANIZATION(S) THAT PREPARED THIS DOCUMENT

**SRI International  
Lockheed Martin Company**

## **ORDERING INFORMATION**

Requests for copies of this report should be directed to the EPRI Distribution Center, 207 Coggins Drive, P.O. Box 23205, Pleasant Hill, CA 94523, (800) 313-3774.

Electric Power Research Institute and EPRI are registered service marks of the Electric Power Research Institute, Inc. EPRI. POWERING PROGRESS is a service mark of the Electric Power Research Institute, Inc.

Copyright © 1999 Electric Power Research Institute, Inc. All rights reserved.

# CITATIONS

---

This report was prepared by

SRI International  
333 Ravenswood Avenue  
Menlo Park, California 94025-3493

Lockheed Martin Company  
3251 Hanover Street  
Palo Alto, California 94304-1191

Principal Investigators

N. Jevtic  
J. Pronko  
M.C.H. McKubre  
S. Crouch-Baker  
F. Tanzella  
B. Bush  
M. Williams  
S. Wing

This report describes research sponsored by EPRI.

The report is a corporate document that should be cited in the literature in the following manner:

*Development of Energy Production Systems from Heat Produced in Deuterated Metals:  
Volume 2*, EPRI, Palo Alto, CA: 1999. TR-107843-V2.



# REPORT SUMMARY

---

EPRI sponsored an experimental program to investigate the idea that heat and possibly nuclear reaction products could be created electrolytically in palladium lattices. Excess heat—which occurred in a number of cases when certain criteria were satisfied—was too large to result from any chemical or metallurgical transformation in so small a mass of material. By inference, some type of nuclear reaction was the hypothesized heat source. This report details the search for “signature” emissions of possible nuclear reactions associated with heat production.

## Background

Palladium (Pd) cathodes electrochemically charged with deuterium (D) to unusually high D/Pd atomic ratios have exhibited episodes of excess heat beyond all inputs. To confirm the suspicion of a possible nuclear reaction producing the excess heat, investigators instrumented operating cells to observe common emissions expected from such reactions, namely gamma rays and neutrons. Volume 1 of this report documents attempts to measure stable helium-4, also a prime suspect among possible nuclear reaction products.

## Objectives

- To measure suspected low levels of gamma rays and neutrons during the episodes of excess heat production.
- To confirm these emissions as signatures of possible nuclear reactions associated with excess heat production.

## Approach

The project team designed a set of electrochemical cells that could be simultaneously measured for excess heat production and gamma ray emissions using calorimetry and gamma spectroscopy, respectively. They also built a neutron detection system for observing low level neutron emissions from possible nuclear reactions. However, they implemented only the gamma ray monitoring of active cells.

## Results

No definitive emissions of gamma rays were detected during attempts to induce excess heat episodes in the detection chamber of the gamma ray spectrometer, possibly because the excess heat episodes did not occur during the gamma ray observation period. The only result of note occurred following a loss of electrolyte incident in which the highly loaded palladium cathode was exposed to the vapor phase of the calorimeter cell. This event resulted in rapid deloading of the exposed part of the cathode accompanied by a rise in temperature from recombination of electrolysis gases at the cathode surface. In this case, a gamma ray of 342 keV associated with the nuclide Ag-111 appeared at a level just above the background.

---

## **EPRI Perspective**

The conflicting requirements of measuring low level gamma ray emissions and assuring precise calorimetry of operating electrochemical cells appears to have defeated the attempt at a simultaneous measurement of gamma rays and excess heat. Gamma emission from radioactive nuclides, reported to EPRI privately by K. Wolf (Cyclotron Institute, Texas A&M), suggested that investigators might observe similar events, though not associated with episodes of excess heat. The appearance of Ag-111 may be such an instance. It is curious, however, that Wolf observed the gamma rays following a temperature transient purposely induced in the electrochemical cell and simultaneously noted low levels of neutron emission. Still, it appears that the correlation of excess heat and a nuclear signature awaits the reliable reproduction of excess heat of sufficient magnitude to justify and warrant a nuclear source. Related EPRI reports address the Development of Advanced Concepts for Nuclear Processes in Deuterated Metals (TR-104195) and Cavitation-Induced Excess Heat in Deuterated Metals (TR-108474). Also available are Proceedings: Fourth International Conference on Cold Fusion (TR-104188, Vols. 1-4).

## **TR-107843-V2**

### **Keywords**

Electrochemical power generation  
Palladium  
Heavy water  
Deuterium  
Cold fusion  
Heat source independent

## ABSTRACT

---

Since the 1989 announcement of the appearance of excess heat in palladium cathodes electrolyzed in heavy water electrolyte, the research has been plagued by intense controversy. The idea that fusion of deuterium could be performed in such a simple room-temperature experiment violated the rules of nuclear physics learned over the past 60 years. The excess heat observed in this work (detailed in Volume 1) was subjected to monitoring of expected products of nuclear reactions, namely gamma rays and neutrons. As it turned out, only the gamma ray monitoring of active cells was implemented. The constraints of the demands of gamma counting and precision calorimetry were too great for a successful outcome in this work. However, an apparent appearance of a radioactive species, Ag-111, detectable by its 342 keV gamma ray, may be similar to emissions observed by Wolf in 1992. In both these cases, heat, if being produced, was not being monitored at the time.



# CONTENTS

---

<b>1 INTRODUCTION</b> .....	<b>1-1</b>
<b>2 NUCLEAR DETECTION</b> .....	<b>2-1</b>
Overview .....	2-1
Gamma and X-ray Spectroscopy .....	2-2
Considerations that Determine System Parameters .....	2-2
Hardware .....	2-4
Detector System .....	2-4
HPGe Detector .....	2-4
Preamplifier and HV Filter .....	2-6
Compton Suppression NaI(Tl) Annuli .....	2-6
The Need for Compton Suppression .....	2-6
Compton Suppression Limitations .....	2-7
NaI(Tl) Round Compton Suppression Annulus and NaI(Tl) Plug Detector .....	2-7
“Square” Annulus .....	2-7
Passive Shielding .....	2-8
Low-activity Lead Shielding .....	2-8
Detection System Configuration, NIM Electronics and Power Supplies .....	2-8
System Configuration and Block Diagram .....	2-8
Power Supplies .....	2-10
Pulse Processing and Shaping .....	2-10
Pulse Height Analysis .....	2-10
Timing .....	2-10
Data Acquisition .....	2-11
Software .....	2-11
Maestro II MCA Emulation Software Data Acquisition .....	2-11
Data Processing .....	2-11
Data Analysis .....	2-11

---

Maestro II MCA Emulation Software .....	2-11
Omnigam Advanced Gamma-Ray Spectrum Analysis Software.....	2-12
Libraries .....	2-12
Programs .....	2-12
ULI.EXE .....	2-12
AN1.EXE .....	2-13
CLB.EXE .....	2-13
CONVERT.EXE.....	2-13
PEAKPLOT.EXE .....	2-13
Developed Software Packages .....	2-14
Counting and Analysis Procedure .....	2-14
Calibration .....	2-14
Calibration Procedure .....	2-14
Sample and Calorimeter Introduction .....	2-15
Data Handling .....	2-15
Spectrum Inspection .....	2-15
Modes of Operation .....	2-16
Geometry .....	2-16
Sample Counting.....	2-16
On-Line Active Calorimeter-Cell Monitoring .....	2-16
Compton Suppressed vs. Non-Suppressed Operation .....	2-17
Detector-Annulus Combinations.....	2-17
System Performance .....	2-17
Detector Efficiency vs. Energy .....	2-17
At Detector-Sample Counting Configuration.....	2-19
At the Position of a Cathode in a Live Calorimeter for On-Line Active Calorimeter- Cell Monitoring .....	2-19
Detector FWHM vs. Energy.....	2-19
Non-Compton Suppressed Operation vs. Compton Suppressed Operation .....	2-19
2-5 Background .....	2-19
<b>3 RESULTS .....</b>	<b>3-1</b>
Strategy .....	3-1
Early Results (Old and New Laboratory -NaI(Tl) Detector).....	3-1
Sample Counting 1 .....	3-2

---

Set-up, Initial Testing and Stability Check .....	3-2
Sample Counting 1 .....	3-2
Cell Experiments .....	3-3
Sample Counting 2 .....	3-4
Sample Counting 3 .....	3-4
Air Cooled Seebeck Calorimetry .....	3-5
Possible Ag-111 Identification During the A1 Run.....	3-7
Gamma Counting.....	3-10
Stand-alone NaI(Tl) detection System .....	3-12
NaI(Tl) Detector .....	3-12
Electronics, Data Acquisition and Handling.....	3-13
<b>4 FAST NEUTRON SPECTROMETER.....</b>	<b>4-1</b>
Detection System .....	4-1
Dual NE-213 Neutron Detectors.....	4-1
Active Cosmic Ray Suppression .....	4-1
Passive Shielding (Thermalization) .....	4-1
NIM-CAMAC Electronics and Power Supplies.....	4-1
Data Acquisition and Software.....	4-2
<b>5 CONCLUSIONS.....</b>	<b>5-1</b>
<b>6 GLOSSARY AND DEFINITION OF ACRONYMS.....</b>	<b>6-1</b>
<b>A APPENDIX A: SUMMARY OF THE OBSERVATIONS AT TEXAS A&amp;M BY KEVIN WOLF .....</b>	<b>A-1</b>



# LIST OF FIGURES

---

Figure 2-1 The GMX Compton Suppressed Detector .....	2-5
Figure 2-2 Compton-Suppressed Gamma Ray Spectrometer Block Diagram.....	2-9
Figure 2-3 Square (no CS) vs. Round Annulus.....	2-18
Figure 2-4 Compton Suppression Effect on Background Spectrum .....	2-20
Figure 2-5 Detection Limit as a Function of Energy .....	2-22
Figure 3-1 Appearance of the 342 keV Gamma of Ag-111 .....	3-8
Figure 3-2 Appearance of the Doublet Nature of the Ag-111 Peak .....	3-11



## LIST OF TABLES

---

Table 2-1 Manufacturer Specifications for the HPGe Detector when Operated with a 6 Microsecond Amplifier Time Constant.....	2-4
Table 3-1 (d,n) reaction Q values for d on the natural Pd isotopes .....	3-9



# 1

## INTRODUCTION

---

An experimental program sponsored by EPRI was undertaken at SRI International to investigate the idea that heat, and possibly nuclear reaction products, could be created in palladium (Pd) lattices under conditions achievable in electrolytic cell experiments. Several types of experiments were performed to determine the factors controlling the extent of deuterium (D) loading in the Pd lattice on the implicit assumption that extremely high loading was essential to the appearance of excess heat and nuclear reaction products.

Following the results reported in 1989 by Fleischmann, Pons, and Hawkins (1-1), considerable effort has been expended to test the hypothesis that the electrochemical loading of deuterium into palladium lattices leads to the production of more energy than is predicted to arise from known chemical or electrochemical phenomena. In the period 1989 to 1992, work was performed at SRI International to confirm the reality of excess heat production. The results of that study have been previously reported (1-2).

In brief, this earlier study confirmed the observations of Fleischmann Pons and Hawkins in that excess heat was observed in amounts far larger than any known chemical process within so small a mass of material. However, the excess heat was observed only when certain criteria were met: deuterium loadings in excess of 0.9 atoms of D per Pd atom; cathodic currents above a threshold value; and satisfaction of an "incubation" time of several hundred hours. A fourth condition discovered later was the apparent need for a flux of deuterium atoms across the cathode surface above a threshold value.

We were unable to account for the excess heat by any artifact known to us and were forced to conclude that the source of the excess power is a property of the D/Pd system. Further, we could not account for the measured excess energy by any chemical or metallurgical process with which we were familiar.

Encouraged by the calorimetric results obtained during the period 1989-1992, it was decided to continue the investigation. However the emphasis for further work was upon attempting to measure directly any species that could be the result of heat-producing nuclear reactions. This report describes the effort applied to observe gamma rays that might be emitted during such nuclear reactions. Attempts to measure stable helium-4, also a prime suspect among possible nuclear reaction products, is described in the first volume of this two-volume final report (1-3).

The approach used in this study was to attempt simultaneous measurement of excess heat and gamma rays. In addition, cell cathodes and electrolytes were analyzed ex situ for tritium and any radioactivity that might emit gamma rays. Although a neutron detection system was built, early termination of the project prevented its use in a significant experiment.

The experiments were carried out in a purpose-built laboratory. This facility was constructed to enable experiments involving potentially explosive mixtures of deuterium and oxygen to be carried out safely and efficiently.

- 1-1. M. Fleischmann, S. Pons and M. Hawkins, "Electrochemically Induced Nuclear Fusion of Deuterium", *J. Electroanalytical Chemistry*, 261, (1989) p. 301 and errata 263, (1989) p. 87.
- 1-2. McKubre, M., Crouch-Baker, S., Tanzella, F., Smedley, S., Williams, M., Wing, S., Maly-Schreiber, M., Rocha-Filho, R., Searson, P., Pronko, J., and Kohler, D., "Development of Energy Production Systems from Heat Produced in Deuterated Metals", EPRI Report TR-104195, September 1994.
- 1-3. McKubre, M., Crouch-Baker, S., Hauser, A., Jevtic, N., Smedley, S., Tanzella, F., Williams, M., Wing, S., Bush, B., McMahan, F., Srinivasan, M., Wark, A., and Warren, D., "Energy Production Processes in Deuterated Metals", EPRI Report TR-107843, Volume 1, June, 1998.

# 2

## NUCLEAR DETECTION

---

### Overview

Since the initial Pons and Fleischmann announcement, considerable effort has been expended to investigate the possible link between the reported excess heat and its possible nuclear origin. Approaches with the highest probability of success in such a search are determined by the probability of emission of a certain type of radiation and the ease and reliability of detection.

Gamma rays are ubiquitous in nuclear reactions and due to the sophistication of gamma ray detection equipment and the ease with which gamma rays traverse matter, they are a natural choice in the search for the link between excess heat and a nuclear signature.

Neutrons are a signature of many nuclear reactions, including D+D and D+T fusion reactions, and are a primary nuclear product to search for in any situation where fusion by these two reactions and possibly others is expected to occur.

Thus, our initial strategy in the search for a nuclear signature of cold fusion placed the focus on gamma-ray/X-ray and neutron detection. However first priority was given to gamma ray detection since others had pursued the neutron detection method and shown the levels to be extremely low.

Thus, a new nuclear laboratory was equipped and instrumented at SRI with a primary function of establishing a correlation between observed excess heat and a nuclear signature. Two major systems, a Compton suppressed high-purity intrinsic germanium (HPGe)-based gamma-ray spectrometer and an actively and passively shielded fast-neutron spectrometer have been built. In addition, we acquired a stand-alone NaI(Tl) detector based gamma spectrometer which allows for the monitoring of whole baths and smaller bench-top experiments.

The HPGe based gamma-ray spectrometer and the fast neutron spectrometers were designed primarily to observe radiation from on-line live electrolytic cells that are simultaneously monitored for excess power. The NaI(Tl) system with its poorer energy resolution is primarily used to screen and monitor standard mass flow calorimeters in baths or for bench-top work. Two approaches were adopted:

1. off-line screening of many cathodes prior to and after calorimetric experiments for potential induced radioactivity.
2. in-situ operation of calorimeters designed to be run within high-efficiency, high-resolution, low-background detectors.

To date, in view of the fact that the nuclear effort on site started some three years after the calorimetry, a large number of cathodes were collected that were never counted with such a sophisticated system for induced radioactivity. As a result, the counting of used cathodes represents a considerable fraction of the operating time of the germanium-detection system. Many cathodes supplied by other laboratories were included in this counting effort. A prime motivation of this effort was the result achieved by Wolf (2-1) at Texas A&M. Wolf observed some seven different isotopes of silver and rhodium after electrolyzing three cathodes for some 21 days in August and September, 1992. A summary of those results, never officially published, is presented in Appendix A.

For greater efficiency, live cell monitoring and post experiment cathode counting were interleaved. Cathode counting was given lower priority. This resulted in the almost 100% utilization of the capability of the gamma-ray spectrometer.

## **Gamma and X-ray Spectroscopy**

### ***Considerations that Determine System Parameters***

Any attempt to detect the nuclear signature of cold fusion, in view of the very enigmatic nature of the phenomenon, must by definition be very broad based. The unknown scale of events both in terms of the energy range over which the search is to be conducted and the nature of the nuclear signature are decisive in the planning of a strategy of the attempt to identify and quantify a nuclear signature with precision.

The reported intermittent nature of the effect necessitates the use of reliable methods of high accuracy, precision and sensitivity. These are a function of both the efficiency and resolution of the system and the background seen by the detector which sets limits on detectability.

For gamma ray spectrometers, the background is complex. The background consists of both narrow gaussian photopeaks and a continuum. The peaks are due to the emission of the natural radionuclides and cosmic rays and their interaction with the material in the vicinity of the detector and with the detector itself. The continuum is for the most part due to partial deposition of gamma ray energy in the detector via Compton scattering. There are other features such as escape peaks.

The simultaneous measurement of heat and a nuclear signature imposes conflicting requirements. Gamma ray detection is most efficient in the absence of absorption and secondary radiation and the detector should be as close to the source as possible, assuming we are dealing with very low emission levels. On the contrary, heat measurements require a heat transfer medium and/or insulation of significant bulk and mass.

A meaningful compromise is governed by the need for simplicity, with redundant sensing where possible and statistically significant sampling whenever possible.

In practice, our goal became the design of a gamma ray spectrometer that was an efficient detector with good resolution in an environment with the least possible background both in the form of peaks and continuum that would nevertheless allow good calorimetry.

To achieve this goal we chose a high-purity germanium (HPGe) gamma ray detector in a shielded environment and with Compton suppression (CS) inside an annulus that can accommodate an entire calorimetric system. Intrinsic germanium detectors have resolutions (FWHM's) on the order of 2 keV and 1.5 keV at 1332 and 661.6 keV, respectively. This is about 25 times better than the 6% of NaI(Tl) detectors at the latter energy making them a natural choice. The properties and capabilities of HPGe systems are treated extensively in a book by Knoll (2-2).

In addition, modern intrinsic germanium gamma ray detectors are available in relative efficiencies exceeding 120% (compared with standard 3-inch diameter by 3-inch high sodium iodide crystal scintillation detectors, measured at the 1332 keV gamma line from Co-60 decay). As the efficiency scales with size, so does the effective energy range for which a detector can be used. Another advantage is that the larger the detector crystal the more "infinite" it seems to the incoming radiation, resulting in more efficient photoelectric deposition of energy versus Compton scattering, and a better peak-to-Compton ratio. Furthermore, thin n-type outer contact coaxial intrinsic HPGe detectors with thin Be windows have effective energy ranges down to 3 keV and hence are X ray detectors as well.

All this led us to select an EG&G Ortec thin window coaxial n-type outer contact HPGe detector in the 50% relative efficiency range of the extra-low background series. All the material that goes into the construction of extra-low background detectors is screened for activity and only material with the lowest possible activity is chosen for such detectors. Efficiency was scaled to give us an upper limit of detectability at least one order of magnitude better than any of the limits on gamma activity set in this field of research to date.

The background is made lower by passively shielding the system from the environment with lead (which as a high Z material is a good absorber of gamma rays) and through the use of active Compton suppression. A NaI(Tl) crystal in the form of an annulus surrounding the active sample or calorimeter, is used to detect gamma quanta that do not photoelectrically deposit all their energy in the germanium crystal. This signal then defines an anticoincident gate.

The Nuclear Instrumentation Module (NIM) standard was chosen for the electronics. A PC-based multichannel analyzer (MCA) emulator was chosen for data acquisition, processing, and first analysis.

In addition to the basic MCA emulation software, analysis software was also acquired that contains extensive radionuclide libraries, allows complex multiplet fitting and considerably simplifies the identification and quantification process. All this together comprises the Gamma Ray Spectrometer currently in operation at the Energy Research Center of SRI International.

## Hardware

A schematic of the detection part of the germanium gamma/X ray spectrometer is shown in Figure 2-1. The system consists of EG&G Ortec HPGe GMX extra-low background detector (1) with the germanium crystal mounted in a cryostat (2) cooled via a copper cold finger from the liquid nitrogen dewar (3), the NaI(Tl) Compton suppression annulus (4) with its 6 photomultiplier detectors (PMT's) (5), the inner bore of which fits snugly around the germanium detector and its NaI(Tl) plug detector at the top (6). The enclosed volume is 260 cubic centimeters (7) and can accommodate an entire calorimeter. All this is encased in a 1721-kg low-activity lead shield (8). The system is located in its own experimental cubicle with a table specifically designed to carry the weight of the Pb (9, 10).

System access is both from the top after removal of the top plates and from the bottom via the hole to accommodate the detector. When the detector is lowered out of the shield it can be moved on tracks to facilitate access. Holes in the lead for cable and tubing access are non-line-of-sight in order not to degrade shielding.

Table 2-1 gives the specifications for the HPGe system used in this work.

**Table 2-1  
Manufacturer Specifications for the HPGe Detector when Operated with a 6 Microsecond  
Amplifier Time Constant**

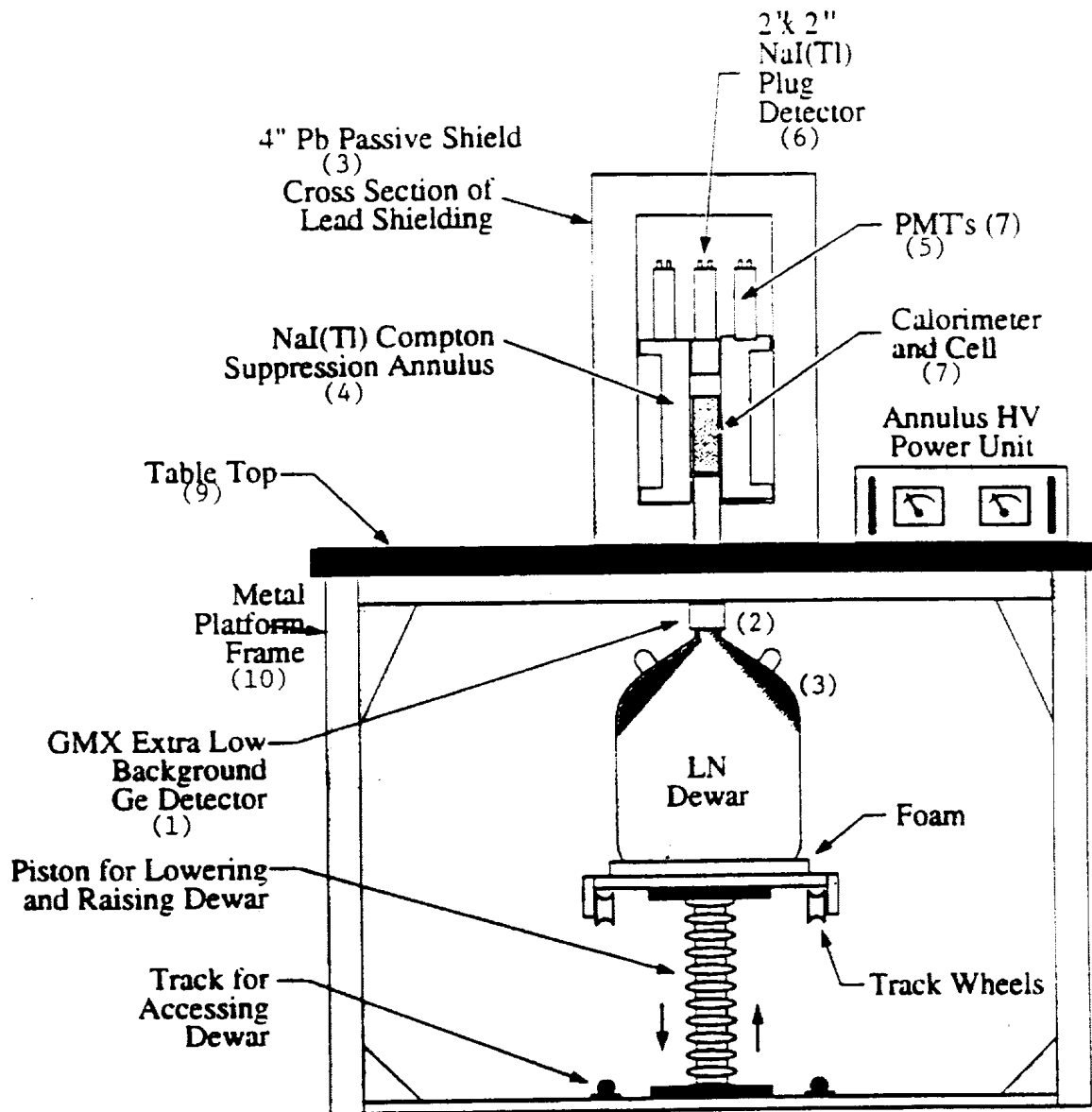
Energy Resolution (Full width at half maximum (FWHM) @1332 keV (Co-60))	2.03 keV
(Peak Integral Counts)/(Compton Continuum Counts) @1332 keV (Co-60)	60.6
Relative Efficiency (as defined above)	52.5%
Photopeak Shape defined as Full width at one-tenth maximum (FWTM)/FWHM	1.95
Energy Resolution at 5.9 keV (Fe-55)	617 eV
Useful Energy Range	3 keV to 10 MeV
High Voltage Bias	3000 volts

## Detector System

### HPGe Detector

The germanium detection system was purchased from EG&G Ortec and is their GMX extra-low background version. The cryostat-dewar system maintains the detector element at high vacuum at close to liquid nitrogen temperature. The dewar serves as a reservoir of liquid nitrogen while the cryostat provides a path for heat transfer from the detector element.

The cryostat provides an outer envelope which can be maintained internally at high vacuum. The cryostat that houses our germanium crystal has a 3.25 inch diameter end cap and is made of specially selected extra low background material. The material of the housing is aluminum that is matched to the thin Be window in terms of thermal expansion.



CM-4035-016

Figure 2-1  
The GMX Compton Suppressed Detector

The vertical streamline configuration was selected in view of the sensitivity of HPGe detectors to vibration and the potential of exposure to vibration while running such cross-disciplinary experiments as simultaneous heat and nuclear measurements.

The crystal is grown from n-type high purity germanium and has a thin n-type outer contact on the closed end coaxial detector. The crystal has a diameter of 65.0 mm and is 65 mm high. The end-cap window made of beryllium (Be) is 0.5 mm thick and is mounted 4 mm from the surface of the crystal.

### ***Preamplifier and HV Filter***

Though a part of the electronics and HV circuitry, the hybrid pre-amplifier (137CN2) and Model 138 high voltage filter are located inside the cryostat. Parts of the pre-amp are cooled with the crystal. The conversion gain of this system is nominally 400 mV/MeV with a negative output pulse signal. The rise time of this tail pulse is on the order of 25 ns with a maximum output of -10 V. Integral and differential nonlinearity is <0.05% over 90% of the dynamic range of the preamplifier.

### ***Compton Suppression NaI(Tl) Annuli***

#### **The Need for Compton Suppression**

In an ideal detector, the only interaction desired would be one full-energy peak such as is observed in photoelectron absorption. However, in real detectors of finite size in addition to each photopeak one observes a continuum that is due to Compton single and multiple scattering. This continuum starts at the Compton edge where the gap between the maximum energy of a Compton recoil electron and the incident gamma ray energy tends to 256 keV for gamma energies much greater than 256 keV.

The fraction of the quanta depositing their energy in the photopeak to the fraction being scattered decreases with energy. When a number of higher energy peaks are present, these continua sum and the resultant spectra are characterized by prominent continua that can obscure low-intensity peaks.

One method to diminish the continuum relative to the photopeaks is by Compton rejection by blanking all counts in the HPGe whenever a Compton-scattered gamma ray is counted by the NaI(Tl) annulus. As mentioned above, the Compton continuum in germanium detectors is generated primarily by gamma rays that undergo one or more scatterings in the detector and that then escape from the crystal. Full energy absorption events do not result in escaping photons. Therefore, coincident detection of the escaping photons in a surrounding annular detector can serve as a means to reject those events that would contribute to the continuum without affecting full-energy deposition events. This signal triggers an electronic gate that is closed if a coincident pulses are detected from the surrounding annulus detector and from the germanium detector.

For Compton suppression to be effective, the gate signal detector, the annulus, must be large enough to intercept most of the escaping photons and efficient.

## **Compton Suppression Limitations**

If a radioisotope has a complex decay scheme, many gamma rays are emitted. The different gamma rays from simultaneous disintegration paths may interact with both detectors resulting in gating on each of them. As a result a large fraction of these events are then rejected, leading to unwanted suppression of full-energy peaks. Consequently for radionuclide identification where relative intensities are the deciding factor it is necessary to run both suppressed to detect weak radionuclides and un-suppressed to make identification easier. Pair production events followed by the escape of one or both of the annihilation photons are also suppressed because either of the two 511 keV quanta can gate off the system.

Compton suppression is sensitive to geometry i.e. the position of the source. It is also sensitive to absorption of the direct and the scattered quanta. Unequal absorption will change gating efficiency. This in turn entails the determination of a background for each geometry and system composition.

From a practical standpoint, drifts in the electronics and intermittent ground loops increase the need for Compton suppression checks and retuning which is a time consuming procedure.

## **NaI(Tl) Round Compton Suppression Annulus and NaI(Tl) Plug Detector**

The NaI(Tl) Compton suppression annulus is the Bicorn model 9HW12/(6)2L-X. It is a 12" long detector that consists of 2 cylindrical NaI(Tl) crystals axially positioned on end and optically integrated at the boundary. It has a 3.35" Diameter axial central cylindrical through-well that is designed to accommodate the germanium detector at the bottom and is closed at the top by a plug detector with a top flange that fits the annulus. The NaI(Tl) annulus is 3" thick and has an outer diameter of 9". The well liner is 0.010" thick Al and the housing is .125" Al with 1.125" top and bottom plates. In effect, in all directions except at the bottom the minimum thickness of NaI(Tl) seen is 3 inches.

Scintillation in the NaI(Tl) is detected by 6 ADIT B50B0 2" 10-stage PMT's that are located in a circle around the well on the top of the annulus.

The resolution of the sum signal for a 661.6 keV Cs137 source on the axis of this annulus is 11%. With the germanium detector in the counting position, the efficiency of the annulus at 661.6 keV is 48.20%. The background in the lead shield from 80 keV to 2.5 MeV is 30 counts per second (c/s). The resolution of the 3" plug is 6.5% at the above Cs-137 661.6 keV line.

## **"Square" Annulus**

In addition to the above "round" annulus, a second NaI(Tl) annulus, was acquired. This annulus has a 5" square well. It can be used both as a stand-alone detector of high efficiency or in place of the round annulus when counting larger calorimeters. The resolution of the sum signal for this annulus is 13% and has an efficiency of 35.5% for a 661.6 keV source at the center.

## ***Passive Shielding***

### **Low-activity Lead Shielding**

The background that the detector sees limits its sensitivity. The background is due to the natural radioactivity of the constituent materials of the detector and its surroundings. In addition the primary and secondary components of cosmic radiation, and the products of the latter interactions with the material of the detector and the material in its vicinity are a significant component.

Total elimination of the natural background is not possible. However, by carefully choosing the materials used in the construction of the detector and components the line background can be made considerably smaller. Lead shielding is used to shield both from the natural radionuclide gamma rays and from the more energetic cosmic ray gamma background. The best shielding is with low activity lead. A passive 4" thick lead shield with almost 4 pi steradian coverage surrounds the annulus and HPGe detector.

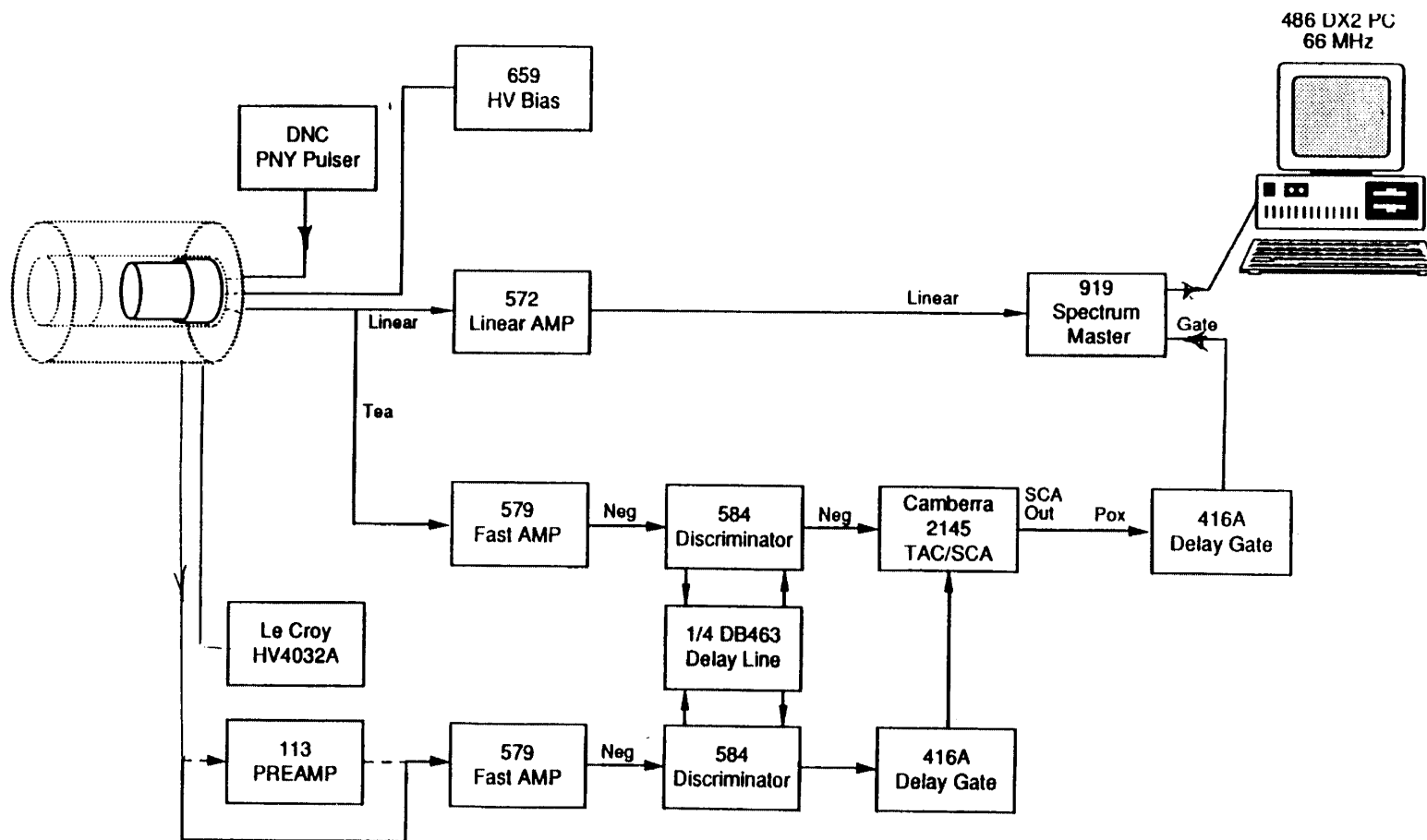
The shield does double duty. It shields the germanium detector and also shields the NaI(Tl) annulus lowering the total background it sees. The background on the unshielded annulus is on the order of 5000 counts/hour due to its large size, hence efficiency. This in turn can lead to spurious gating of the germanium signal.

The total weight of the shield is over 1721 kg. It is made of disks 0.5 inches thick and rings to facilitate stacking and removal. There are 8 disks on the bottom and as many on the top. A hole 3.5" Diameter on the bottom accommodates the 3.25-inch diameter detector capsule. The annulus PMT HV cables and signal cables are brought out through curved channels to minimize loss of shielding efficiency. Though the primary function of the annuli is to serve as source of a timing signal to define an anti-coincident gate, in effect the mass that is thus placed between the detector and the outer world gives it considerable merit as a cascade down shield.

## ***Detection System Configuration, NIM Electronics and Power Supplies***

### **System Configuration and Block Diagram**

The gamma ray spectrometer is a NIM standard system (Figure 2-2). The charge due to the passage of a gamma ray through the germanium crystal has to be collected and integrated and the obtained signal then processed to extract the desired energy data. On the other hand the signal from the NaI(Tl) annulus has to be conditioned in such a way as to give us reliable timing signals for gating. It becomes clear that our electronics will need to perform two different functions. One branch (the slow branch) will be used to extract information on pulse heights i.e. energies of the incoming radiation which will in turn yield the identity of the source of the radiation. The second branch, the fast branch, will have to give us the exact time relationship of two signals, signals which define our Compton suppression gate. This second branch signal has to be delayed in order to reach the MCB gate simultaneously with the spectroscopy signal.



CM-4035-26

Figure 2-2  
Compton-Suppressed Gamma Ray Spectrometer Block Diagram

In addition to the HV power supplies needed to operate the HPGe detector and the annulus PMT's a number of other NIM modules are needed as can be seen in the block diagram of our system, (Figure 2-2). It consists of two branches, the upper yields energy information and the lower performs the timing i.e. gating function. The timing branch itself consists of two legs, one for the germanium start signal for the gate and the other for the NaI(Tl) stop signal.

## Power Supplies

These consist of the germanium detector bias supply-(EG&G Ortec model 659 (with auto shut down)); NaI(Tl) annulus PMT HV power supply-Le Croy system HV4032A with 4 output HV pods. Operating HPGe and tuning NaI(Tl) preamplifier power are obtained from the fast filter spectroscopy and amplifiers.

## ***Pulse Processing and Shaping***

### Pulse Height Analysis

As can be seen in Figure 2-2, the direct or slow branch yields pulse height information. The initial charge collection is done at the detector by the charge sensitive preamplifier in the cryostat housing which also converts the current pulse to a voltage pulse and shapes it. Tail pulses with rise times of 25 ns and fall times on the order of 50 microseconds from this preamplifier are then input into a EG&G 472 spectroscopy amplifier whose basic function is to reshape the signal and amplify it. The result is a signal with a rise time of a few microseconds and slightly longer fall time. This signal is then input to a EG&G Ortec 919 Spectrum Master (Figure 2-2) which is a 4 input multiplexed 16k channel Analog to Digital Converter (ADC). This ADC measures the amplitude of each incoming pulse and generates a digital signal proportional to its height that is then counted in the appropriate channel as a pulse. The ADC is interfaced with a PC via a card which supports the multichannel analyzer emulator.

In addition to the above modules, a BNC PB-4 pulse generator at the HPGe preamplifier test input allows us to monitor the system for stability over long periods of time or to trouble-shoot when needed.

### ***Timing***

The principle of anti-coincidence gating consists of rejecting signals whenever the HPGe detector and the NaI(Tl) annulus see a signal at the same time, or more precisely within a narrow time window. This function is accomplished by the lower branch in Figure 2-2 which has two legs.

The same signal that is fed to spectroscopy amplifier for pulse height analysis is input to the gate start branch. Here the signal is first converted by a EG&G Ortec 579 Fast-Filter Amplifier (FFA) to a fast timing pulse that is then fed to a EG&G Ortec 583 Constant Fraction Discriminator that generates a fast negative NIM output. This signal is first delayed by an EG&G Ortec 416A Gate and Delay Generator and then serves as a start signal for a Canberra 2145 TAC/SCA.

The sum of the signals from the annulus PMT's is fed to an identical FFA-CFD configuration to the one mentioned above then via a EG&G Ortec 416A Gate and Delay Generator to the stop input of the TAC/SCA closing the anticoincident gate at the ADC.

### ***Data Acquisition***

A 486 DX2 66 MHz PC is used for data acquisition. The multichannel buffer and the PC are interfaced via a Ortec PC BCBL1 interface card.

### ***Software***

#### **Maestro II MCA Emulation Software Data Acquisition**

Maestro II MCA Emulation software by EG&G Ortec is used for data acquisition. This is software designed for the Windows platform. It is fast, can be used for multiple output ADC's and as such can support more than one detector. Though this software does not have event-by-event capability, variable length data dumping is possible. JOB programs allow automatic functions and partial system control during data acquisition.

### ***Data Processing***

Maestro II has some data processing capability. JOB programs also allow a degree of automation in processing data. However, Maestro has a major limitation in that though data collection can be followed live, to access analytical functions one must switch to the buffer. No real time updating in the MCB mode is available.

Maestro does not have a spectrum stripper. Some of these shortcomings have been alleviated by a group of programs that were written to complement Maestro capabilities.

### ***Data Analysis***

The analysis procedure combines the capabilities of Maestro II, our own software and the extensive Ortec Omnigam package.

### ***Maestro II MCA Emulation Software***

The capabilities of the Maestro software in the analysis realm are limited. For the most part, for low level work, the Peak Search functions is useless at all sensitivities. At lower energies the software has limited multiplet deconvolution capability. However, for regions of interest set on the basis of a LIB.MCB file a report may be generated that gives integral region of interest (ROI) contents with no deconvolution.

## **Omnigam Advanced Gamma-Ray Spectrum Analysis Software**

This software performs library directed analysis for expected nuclides and peak-search directed analyses for unexpected nuclides. On the basis of efficiency and calibration data it can perform quantitative analysis. The program package consists of libraries and executable programs.

### **Libraries**

The Omnigam package contains extensive libraries. The largest of these are:

1) ESMMASTER.LIB - 1052 nuclides and 12381 peaks with nuclide half-lives greater than 1 minute; 2) .ESSHORT.LIB - 490 nuclides and 4499 peaks with nuclide half-lives less or equal to 10 minutes; 3) LLHPG.LIB - 83 nuclides and 8181 peaks prompt gamma rays from neutron capture; 4) NAC.LIB - decay gamma rays from neutron activation analysis, contains nuclides with half-lives greater than 10 hours.

In addition to the above, the package also contains a shorter general library ENDSF.LIB that contains 352 nuclides and 1536 peaks and no X ray peaks; a natural radionuclide library NATURAL.LIB; a nuclear power plant library NPP.LIB; a food library FOOD.LIB; a detector library DET.LIB; and a suspected nuclide library that contains the five most significant peaks from ENDSF.LIB called SUSPECT.LIB and a MIXCLB.LIB. These libraries contain all the peaks of a certain nuclide that are more intense than 1 gamma per disintegration. All the nuclide uncertainty values have been arbitrarily set at 5%.

For strong sources with lines less intense than 1 gamma/ disintegration one finds recourse in references such as "Tables of the Isotopes" by C.M. Lederer and V.S. Shirley. (2-3).

### **Programs**

In addition to the libraries listed above, Omnigam has a number of very useful programs extending its capabilities far beyond those of Maestro II:

#### **ULI.EXE**

The ULI.EXE program allows us to use above libraries to generate user application libraries. NT.LIB is the background library that contains lines seen in our background. It does not contain any X ray lines below 70 keV and is used for the general inspection of the collected data. Libraries can then be used to generate \*.MCB files which Maestro II uses and are particularly useful if they contain efficiency data. In this manner a useful first iteration report can be generated using Maestro II.

The options are varied and allow for library customizing. However, extensive manipulation is not recommended from within ULI as it takes 8 hours even on the 486 DX-2 66 MHz PC to sort ESMMASTER.LIB. No provision is made for half-life based isotope selection though lines may be organized by isotope or energy.

## AN1.EXE

AN1.EXE uses the spectrum file in the Maestro .CHN format or the Omnigam SPC format and a library specified by the user to yield reports of varying complexity. If no library is specified, a general peak search can be performed using this program. All detected peaks are listed in the generated report as unidentified. When a library is specified, in addition to the unidentified peaks, AN1 does a library directed search for all peaks in the library. If, finally, efficiency calibration data is incorporated into the .SPC file, the program yields the actual activities of the various nuclides, and in their absence, sets upper limits on their activities. AN1 also has the option of multiple library use for the deconvolution of multiplets. The outputs are a report, the .RPT file and a .UFO file used by PEAKPLOT for graphics.

## CLB.EXE

The Omnigam calibration routine is CLB.EXE. It generates a .CLB file. The system may be energy and efficiency calibrated using this routine. This data may then be used to generate libraries with efficiency factors or it can be integrated into the .SPC file. An example of its output is a .PRN file for the counting geometry at the detector. It gives the energy calibration, the efficiency calibration and the FWHM vs. energy. In addition it may be used to transfer an energy or efficiency calibration to a .SPC file or from one file to another. However, one must be careful. The FWHM fit given grossly overestimates the FWHM at higher energies by about a factor of 4. This program demands an understanding of the effects of geometry and should be used with care.

## CONVERT.EXE

The CONVERT.EXE program integrates all the files necessary for an overall analysis generating a .SPC spectrum file that may contain the analysis parameters and efficiency information.

## PEAKPLOT.EXE

The PEAKPLOT.EXE routine is used display and to print the spectra. It aids in fitting by allowing us to better define the libraries used by the AN1 analysis program. It is of great help in the visual deconvolution of multiplets and has hardcopy output of the spectrum fitting results. A plot of FWHM vs. Energy is also a part of this routine.

Libraries defined in the above manner when combined with a .SPC spectrum to which the .CLB file information has been transferred allow AN1.EXE to generate reports which incorporate the efficiency and thus contain the actual activities and upper limits on all the nuclides specified in the library as well as count rates for any other peaks detected.

However, one note of caution is necessary. Omnigam has problems in handling all non-Gaussian peaks whether this be due to the slight asymmetry of the inherent peak shape of the system or to walk (calibration drift during a long run).

## ***Developed Software Packages***

In support of the above, a number of programs were written and program packages developed to facilitate data analysis. These include .JOB and .BAT programs that complement the existing Maestro and Omnigam software. Moreover, various conversion programs in C and C++ were written. Also a novel methodology for predicting the development of low level peaks was developed.

In addition to programs developed, a major effort was made to upgrade the available libraries by including sorting by half-life.

The Maestro program outputs reports that give net counts for user defined regions of interest, the peak centroid and the FWHM and FWTM with ID candidates selected from a user defined library and a corrected rate for that radionuclide.

The Omnigam program has in addition to its capability to resolve multiplets, a multiple report format of increasing complexity. It will give a list of peaks found that are not included in the libraries specified libraries in the “Unidentified Peak Summary”. It will also, if no multiplet deconvolution libraries are specified, list all nuclide candidates for a given line, giving the net counts for one and zeroing the others. This can then be used as a guide how to define the multiplet deconvolution libraries. It will list these and all the library peaks found as well as those with no net counts in the “Identified Peak Summary”. In addition, the “Summary of Nuclides in Sample” gives data on all the nuclides specified in the libraries. For nuclides present, this consists of the activity and for those for which the search was negative, an upper limit is specified. A “Summary of Library Peak Usage” summarizes the methodology used in the calculation.

## ***Counting and Analysis Procedure***

### **Calibration**

A set of gamma ray and an X ray calibration sources were purchased. They included Na-22, Mn-54, Co-57, Co-60, Cd-109, Cs-137 and Fe-55.

### ***Calibration Procedure***

The system is calibrated on a regular basis and whenever any of the system parameters are changed. These included power-downs, gain changes and pole-zeroing on the spectroscopy amplifier. The liquid nitrogen dewar has 32 liter capacity that is usually enough for two weeks of operation. Initially, the system was calibrated after each fortnightly fill for which the detector high voltage was taken down. Over time, a procedure evolved whereby the detector was not powered down during a fill, eliminating the need for a recalibration every two weeks. The stability of the system is such that over a 1 million second (11.6 days) count the change in the FWHM at the 1460 keV K-40 line does not increase in a statistically significant manner.

Due to the very good linearity, the Co-60 and Co-57 sources are used to energy calibrate our system. For an efficiency calibration, a combination of all the sources is used.

## **Sample and Calorimeter Introduction**

As can be seen in Figure 2-1 the samples to be counted are introduced from the bottom. This is done by lowering the detector, placing the samples on top of it and reintroducing the detector into the annulus.

For on-line calorimeter monitoring the system is accessed from the top. The lead disks are removed and the calorimeter lowered and suspended. Initially water cooled heat flow calorimeters were used, the wiring and cooling water piping being introduced through holes in the lead that were designed for the annulus cabling. The design of the calorimeters was later changed to an air cooled Seebeck heat flow type. In this case the air is introduced from the bottom via a collar.

## **Data Handling**

In both the sample counting and the cell-monitoring geometry data is acquired in dumps whose duration could be changed. The duration was chosen in each instance depending on the total background, the half lives of the isotopes to be observed and the suspected activities. The dumping procedure also provides a check on intermittent noise which was a problem encountered a number of times during the period of this report. Dumping allowed us to follow noise onset and time evolution and thus helped us locate a number of external noise sources that were eliminated.

Over time, a series of programs was developed to allow variable length dumps. Shorter dumps were used in intervals during which dynamic phenomena were expected in the system and longer ones in periods when parameter changes were not expected.

## **Spectrum Inspection**

Gamma ray spectra consist of narrow lines and the continuum which is the sum of Compton scattered photons of the lines present. In addition, backscatter peaks may also be observed.

For a structure to qualify as a line it has to satisfy two criteria: (1) that the sum of counts under the peak defined by a region of interest of plus or minus 3 sigma be greater than 3 times the error in net area. (This error is defined as the square root of the sum of squares of the errors of the adjusted gross area and the weighted error of the background) and (2) that the FWHM for a fully developed peak be equal to the value specified by the detector curve of FWHM vs. energy.

However, in practice these two requirements are complementary. Thus shape will allow us to observe peaks smaller than 3 times the error and for low intensity non-fully developed peaks the FWHM requirement is not always fulfilled and may take any value below the calibration value.

Initially a reference spectrum is taken of the background, preferably for the longest feasible time. This spectrum is then quantified in terms of peaks and baseline. These spectra differ for the various configurations of interest and reflect the material seen by the detector. Such background spectra are then the reference to observe novel features. The lines are identified and the appropriate libraries such as NT.LIB are set up to determine activities.

Prior to any inspection, a spectrum is tested for noise. This is the result of early noise problems with the detector. However, for instance, at current operating conditions, with about 32000 counts per 7200 s dump, this gives us a sensitivity of +/- 0.075 c/s which in itself is a crude measure of any activity.

Visual inspection consists of comparison of the spectrum under scrutiny with the “reference” background spectrum. The acquired spectrum is searched for any new peaks of the proper FWHM and the baseline is inspected for broader structures that would indicate particle emission. The general shape of the baseline is verified both to check for the proper functioning of the Compton suppression system and for bremsstrahlung. All background peaks are checked for count rate and some regions, such as the 70 keV to 90 keV region is deconvoluted in search of occluded lines.

If new lines are observed, prior to a detailed spectrum analysis, the respective candidate libraries are compiled. Regions of interest (ROI's) are marked where ever a line is seen and a library directed search is made for all unknown and potentially interesting lines on the basis of first the background library (NT.LIB) and then the current candidate library (CAN.LIB). Whenever necessary, X ray libraries are generated for the region below 120 keV.

The detailed Omnigam analysis is performed if anything noteworthy is observed or if upper limits need to be set.

## **Modes of Operation**

In view of the above, a number of possible modes of operation exist.

### ***Geometry***

#### **Sample Counting**

The most shielded geometry is the sample counting geometry. The detector is brought up from the bottom to half way up the annulus with the sample or samples sitting either on top of the teflon jacket that is used to protect the detector against possible spills or with the samples looking at the Be from an end-cap/holder. In this position Compton suppression for a source at the top of the detector is optimal.

#### ***On-Line Active Calorimeter-Cell Monitoring***

Initially forced liquid convection and later air cooled Seebeck calorimeters were designed that could be introduced into the central hole of the round annulus. With a calorimeter in place, the detector is inserted into the annulus to a lesser degree. Thus, the background in this configuration is considerably higher. In addition, due to the intervening mass for any source at the position of the cathode, the Compton suppression is less effective. Also, the range down to which Compton suppression is effective is at a considerably higher energy, all depending on the specific geometry and materials used in the experiment.

## **Compton Suppressed vs. Non-Suppressed Operation**

As has been mentioned earlier, counting may be done in the non-suppressed mode and the suppressed mode. Suppression occurs at partial deposition of energy in the germanium detector crystal when the detector and the annulus see an event within a narrow time window. In our case this value is 1 microsecond at the TAC/SCA input. Suppression is defined in terms of the peak to Compton ratio which is the ratio of the number of counts in the channel with the maximum number of counts in a well developed peak to the average number of counts in a region below and away from the Compton edge. Our system routinely runs at a peak-to-Compton of 500:1 for the Cs-137 661.6 keV line. For the 661.6 keV Cs-137 line, the energy range of interest is between 358 and 382 keV. Whether Compton suppression is useful depends on many factors. First, for the Compton suppression to be useful, we must be dealing in relatively low activities. For high activities, random gating comes into play and non-suppressed operation is imperative. In addition, cascades where all the members lie in the active suppression range (in our case from 80 keV to about 1 MeV) will result in suppression of all the lines. Thus, the probability of suppression in terms of the energy of the line and its cascade multiplicity and the suppression efficiency and range determine whether suppression is beneficial.

## **Detector-Annulus Combinations**

Throughout the duration of this contract various detector-annulus combinations were used. This was due to noise problems with our GMX detector and problems with the annulus power supply. To date we have run with 3 separate detectors: 1) our GMX extra-low background detector; 2) at different times two POP-TOP capsule low background detectors which were on loan from EG&G Ortec. The two annuli, the round and the square were used at various times.

Whenever data is presented, the actual configuration used will be noted. Comparison of the background in the round annulus with CS and in the square annulus with no CS is given in **Figure 2-3**.

## **System Performance**

A number of parameters are used to characterize a detection system. Of these, the most important are the efficiency and resolution and the background, both continuum and peaked seen by the detector. These in turn define the sensitivity of the system and set the limits of detectability.

## **Detector Efficiency vs. Energy**

Detector efficiency may be defined in various ways. The efficiency quoted henceforth will be the photopeak efficiency, i.e. the total number of counts in the photopeak divided by the activity of the source.

# BACKGROUND

Comparison of "Square"annulus with no Compton Suppression and Round  
Bore Annulus with Compton Suppression

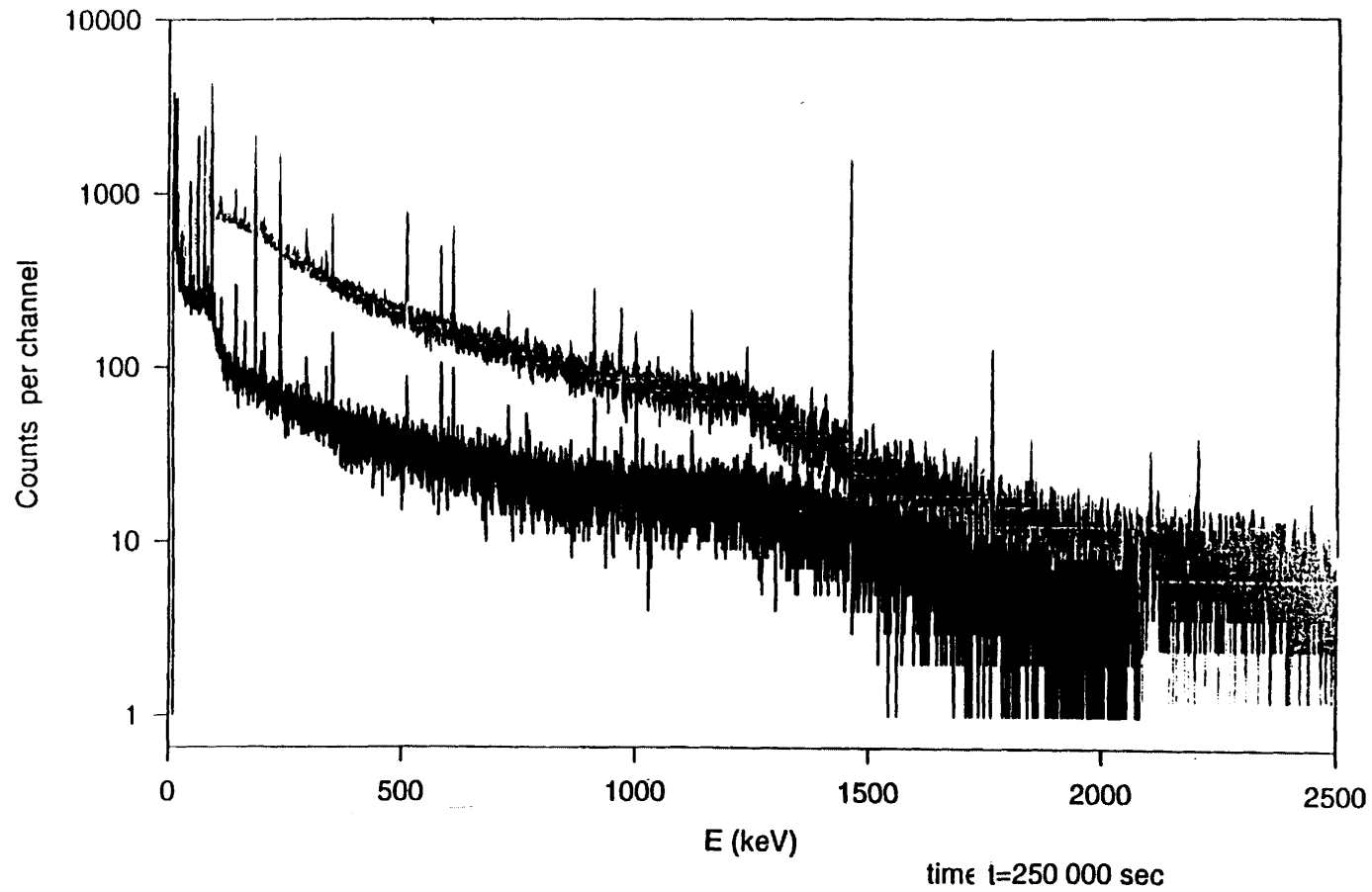


Figure 2-3  
Square (no CS) vs. Round Annulus

### ***At Detector-Sample Counting Configuration***

The detector has two main modes of operation. The detector efficiency is in the 10% range below the knee and drops to about 1% at the 1332 keV line with a knee at about 200 keV.

### ***At the Position of a Cathode in a Live Calorimeter for On-Line Active Calorimeter-Cell Monitoring***

For the case of a cell in an air Seebeck calorimeter the efficiency at the detector which is pertinent to on-line calorimeter monitoring at 122.08 keV is down to 1/24 of the value at the detector for close in sample counting. Of this 23 parts is distance and 1 part material absorption. At the Pd K X line of 21.12 keV this becomes 1/80.

### ***Detector FWHM vs. Energy***

The resolution varies from 0.89 keV at 122 keV to 1.5 keV at 661 keV to 2 keV at the higher Co-60 line of 1332 keV.

### ***Non-Compton Suppressed Operation vs. Compton Suppressed Operation***

A comparison for the case of cell monitoring geometry of the background with and without Compton suppression is given in **Figure 2-4** (sumodd - sumeven) at a suppression of 500:1. The effect in terms of the detection limit is a halving of the background full scale. The effect of the suppression is best appreciated in the fact that for our GMX detector the non suppressed spectrum continuum represents ~95% of the counts seen. This reduction of the background by 30% increases the fraction of the counts in the peaks to almost double.

For the cell monitoring geometry, however, Compton suppression efficiencies drop significantly. This is both due to the fact that the detector in this mode is positioned at the bottom of the calorimeter with a less favorable geometry for collecting the Compton scattered gamma's. In addition to the change in scattering angle entrance cone, the material of the cell plus calorimeter also contributes to poorer suppression.

In addition, it was concluded that the plug detector contribution to Compton suppression is negligible in our cell counting geometry and almost so in the sample counting geometry. Furthermore, when the annulus was sent back for PMT replacement, a gain mismatch was introduced making it even less useful. This justifies the use of the plug as a stand alone detector.

## **2-5 Background**

The end result of all the measures taken is a background that gives a limit of detection for a long spectrum with no noise at the low end of  $10^{-3}$  c/s at 30 keV and  $10^{-4}$  c/s at 1.3 MeV. Although there are over 100 potential lines in a spectrum in the sample counting geometry, the total number of lines above 3 sigma for a counting time of 720 000 seconds that also satisfy the FWHM criterion and have ID's is 29.

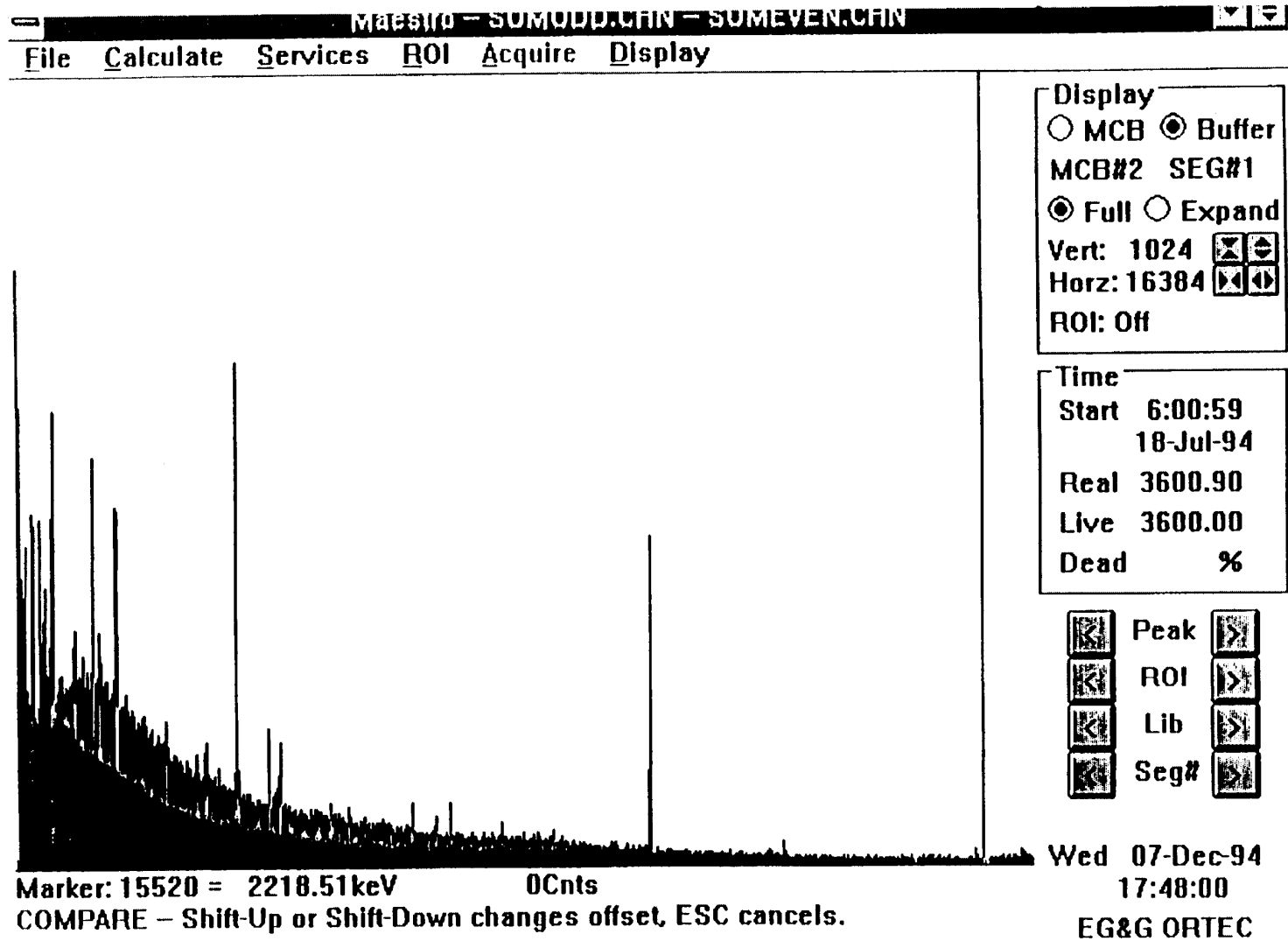


Figure 2-4  
Compton Suppression Effect on Background Spectrum

The convolution of the efficiency curve and the effect of the background continuum is given in **Figure 2-5** for the case of a counting run of 1.08 million seconds taken over the 1994 Christmas holidays. The system was running at a CS of 300:1. To estimate the background continuum contribution, all the peaks were first subtracted from the spectrum, then the spectrum was scanned by a ROI defined by the curve and  $\pm 2.5$  times the FWHM at that energy. This total area is then used to define the error on the spectrum as 3 times its square root. Due to the slow variation of the continuum and the narrowness of the lines this curve was obtained by an approximate method. The error is estimated at 2.5%. This curve exhibits a local maximum at the lowest energies which is due to a recurrence of noise on the system. Then it dips to a minimum at about 240 keV. To this energy, due to the constancy of the efficiency, the curve barely reflects the background. After the minimum, the detection limit curve has the appearance of a line with positive slope. This is due to the combined effects of the shape of the efficiency curve, the background, and the Compton suppression. After about 1 MeV the slope of the curve increases. At about 1400 keV the background diminishes considerably and the end of the curve is due to the precipitous drop in efficiency. The bumpiness of the curve is due to the smoothing, averaging and rounding off procedures used and is an artifact of the processing.

A comparison of the background seen by the unshielded detector, with it inside the NaI annulus but with no lead shielding and inside the annulus with lead shielding but no Compton suppression for 71 000 s results in a total number of counts over the whole range of 7,558,269, 2,177,725 and 377,353, respectively. These reduce to 106 c/s, 30.67 c/s and 5.24 c/s.

It is safe to say that for the very long background counting runs, in the sampling geometry, the major contribution to the line spectrum is due to the activity present in the detector components and Compton suppression is efficient. In the cell monitoring geometry, the detector sees more background due to its poorer shielding. Also we do not screen calorimeter materials for low activity and they introduce a background too. All this contributes to a substantially reduced effect of the Compton suppression during live cell monitoring.

A comparison of a Compton suppressed and a non-Compton suppressed spectra was shown in Figure 2-4.

The background library NT.LIB was developed over time. It contains 43 entries of which 28 are radionuclides from the natural radioactive chains for a total of 177 peaks, the Pb L X-ray peaks (5) and the U K X-ray lines (4) and entries that correspond to the Pb, Tl and Bi K X-ray lines.

In addition to the radionuclides and lines listed above, this library contains lines that are the result of thermal neutron capture on Ge-70 at 198.4 keV and on Ge-74 at 139.9 keV and an inelastic neutron scatter structure on Ge-72 at ~691.3 keV and on Ge-74 at ~596 keV.

2-1. Wolf, K., Private Communication, 1992

2-2. Knoll, G.F., Radiation Detection and Measurements John Wiley and Sons, (1989)  
QC787.C6K56 and ISBN 0-471-81504-7

2-3. Lederer, C., and Shirley, V., Browne, E., Dairiki, J., and Doebler, R., Shihab-Eldin, A., Jardine, L., Tuli, J., and Buyrn, A., "Table of Isotopes", Seventh Edition, John Wiley and Sons, New York, 1978

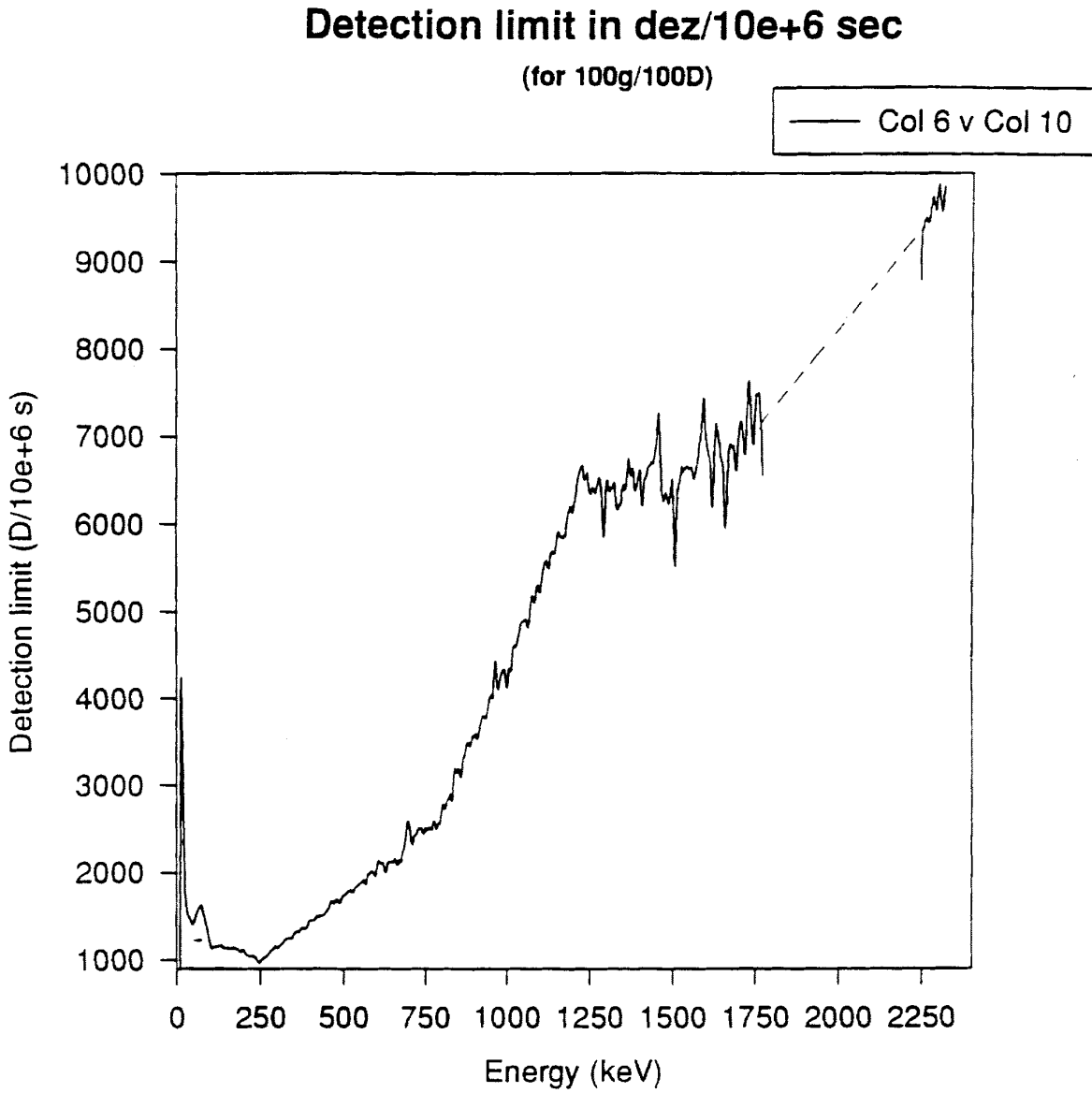


Figure 2-5  
Detection Limit as a Function of Energy

# 3

## RESULTS

---

### Strategy

The objective of the nuclear effort is to establish a correlation between heat and a nuclear signature. At the same time, no effort was spared to search for nuclear events not related to heat measurements.

In view of the fact that the nuclear effort on site started three years after the calorimetry, a large number of cathodes that were run in electrolytic cells, some of which gave excess power were not counted prior to August of 1993. As a result, the counting of used electrodes represents a considerable fraction of the operating time of the germanium detection system to date.

The timeline of bringing up the new laboratory will at times be referred to insofar as it pertains to presented results. This is particularly true for live calorimeter monitoring as it was necessary to develop a reliable calorimeter design that would give calorimetric results of satisfactory accuracy in a system to which access was difficult and of which no visual inspection was possible. This will be dealt with in detail elsewhere. Suffice it to say here that the initial design of a water cooled heat flow calorimeter with a teflon body and a cylindrical envelope for forced liquid cooling evolved to an air cooled heat flow Seebeck calorimeter with Degree of Loading (DOL) glass cells and cooling fins. All versions used in front of the germanium detector had cathode resistance measurement to determine D/Pd loading.

Before presenting the germanium detector results we will briefly dwell on the measurements conducted in the initial phases and while the new laboratory was being built and equipped.

### Early Results (Old and New Laboratory -NaI(Tl) Detector)

Prior to the purchase of the equipment for the Compton suppressed gamma ray spectrometer, the move to the new laboratory and the operation of the new equipment in it, a series of measurements was conducted with equipment available on site here at SRI.

These measurements were conducted using a 2 x 2" NaI(Tl) Bicron detector with an integral preamplifier base and initially a Canberra Series 40 Multichannel Analyzer. Later the Canberra was replaced by a EG&G Ortec 372 Spectroscopy amplifier and a PC based Maestro MCA emulator. An Ortec HV power supply was used throughout.

During this period, starting in September of 1993, two types of measurements were made. First and foremost, the NaI(Tl) detector was used to monitor possible activity in the T series of experiments (T-1 to T-4). In parallel with the above measurements, and interleaved with them, a

series of materials and electrodes were counted. The detector was exposed to the total background in the former case. In the latter case, lead shielding was used to reduce background which was as low as 2 c/s in the range from 70 keV to 2.5 MeV.

Nuclear monitoring of T-1 was started Sept. 18, 1993 ending with T-4 on March 22, 1993. These were monitored in a water bath with the NaI detector viewing the calorimeter through the outer bath wall. T-1 and T-2 were prototype trial runs. T-3 and T-4 had temperature sensing capability. The thermal anomalies observed in T3 are discussed elsewhere (1-3). The efficiency during T-4 monitoring was three orders of magnitude of that at the detector due to the intervening material and distance. No gamma ray activity above background was detected in the 70 keV to 5 MeV range over this period. This, in view of the difficulty in quantifying the thermal anomalies observed, does not allow us to set upper limits on the excess heat vs. nuclear activity correlation.

In parallel with the above measurements, and interleaved with them, a series of materials and electrodes were counted. These included samples from R. Oriani, a 3 mm Engelhard cathode, virgin Tanaka foil prior to and after the T series runs and the cathodes from P2, P12 and P22 (1-2). These samples were counted in a lead shield of up to 4" thick and positioned at the face of the detector. No activity above background was detected on any of them.

## **Sample Counting 1**

### ***Set-up, Initial Testing and Stability Check***

Following the move to the new laboratory, the germanium detector became operational at the end of January, 1993. Originally, a 92X Spectrum Master Gamma Spectroscopy Workstation that incorporates detector power, pre-amp power, a spectroscopy amplifier and the MCB was purchased. However, initial testing showed that the unit had a stability problem and it was exchanged in February of 1993 for a 919 Spectrum Master 4 input Multichannel Buffer and a 672 Spectroscopy amplifier. This configuration satisfied our stringent demands for stability. The system is currently being run in this second configuration.

During this time the lead shield for the system was designed and machined. Also, the various modules were tested. Due to a backlog at Bicron, the NaI(Tl) annulus was delivered in March of 1993. The Compton suppression annulus was integrated into the system during April of 1993 with a maximum Compton suppression of 700 to 1.

### ***Sample Counting 1***

After initial trial runs, two sets of samples were counted in the counting geometry. The first set of samples was an extensive collection of material used in the early cold fusion experiments and archived at Rockwell International. No activity above background was detected though Co-60 contamination was in evidence.

The second was a set of samples that were sent to us by K. Wolf (Cyclotron Institute, Texas A&M) (3-1). These samples included samples of different histories. The samples were first counted together, then in groups. One sample was an electrode that had been used in the Kamiokande experiments whose history was not well known. This sample was heavily contaminated by Am-241. No activity above background was detected from the rest of these samples. Of particular interest were two samples. These are two halves of a 4 cm cathode that was one of four electrodes run in the Black Cloud Mine experiment. Four such electrolytic cells had been running at the time when excess neutrons over background neutrons were detected. One of these halves subsequently first produced 3-4% and then 1-2% excess power when run in two closed calorimeter experiments. A Seebeck isothermal heat flow calorimeter was used and over six months elapsed time separated the two calorimetric runs. However, as the experiment at the Black Cloud Mine was conducted with 4 cells running simultaneously, the probability that we were counting the neutron producer is 0.25. As a result, no meaningful limits can be set nor a satisfactory correlation postulated between neutron emission, heat production and gamma activity in this case.

This series of sample counts was also of interest in that this was the first time we could observe the effect of a large mass of Pd in front of the detector. The Pd KX line which consists of the K alpha-1 at 21.177 keV and K alpha-2 at 21.02 keV. The line was observed when a large mass was present and when foils were counted.

In addition, the practice was instituted to count electrodes from calorimetric experiments just after a calorimetric run ended, resulting in some 20 L Series and 4 M series cathodes being counted.

## Cell Experiments

The G cell calorimeter was a design optimized to allow the simultaneous monitoring of both excess heat and gamma ray activity and is described in V.1 of this report (1-3). It was a forced liquid convection cooled design and was sized to fit inside the NaI(Tl) Compton Suppression annulus. The bottom of the cell was made of thin PTFE with a Al cooling jacket to minimize absorption both in the line of sight of the GMX detector and for Compton scattering.

Four experiments were conducted, with each successive calorimeter evolving from the previous. The G1 to G4 series of experiments were run from July 1993 through February 1994. The electrochemical aspects and the calorimetry of these experiments are dealt with elsewhere (1-3). The calorimeters themselves were designed as a reflection of the calorimeters actually used in experiments that yielded excess power. The complexity of mating calorimetry and on-line gamma detection, of fitting a calorimeter into a 3.5" diameter space and the need to up-scale resulted in a rapid evolution of the design. The G1 and G2 were crown cathodes as in C1 with good aspect ratios vis a vis the germanium detector. These cells had double cylindrical nickel anodes. The experience with loading cathodes in the presence of Ni anodes prompted a return to Pt anodes. The loading of both of these cathodes fell short of the required 0.9 for excess power generation. Cells G3 and G4 were a return to the standard rod cathode geometry with a single anode. The G3 and G4 cells were used to test the assumption that deuterium flux across the cathode surface will result in heat generation. G3 was cycled stepwise between positive and negative currents but no calorimetric data could be obtained while in this mode. This cathode achieved a high loading of 0.91 which was maintained for a 46 hour period during which it was not cycling. No excess power was observed during this interval.

Calorimeter G4 was run with an axial current of up to 7 A. No cathode loading data is available in this regime. No excess heat was observed with a calorimetric uncertainty of +/- 50 mW.

During this set of experiments, data was taken in 15-minute intervals. The advantage of these short dumps became a necessity when a noise problem was encountered with the germanium detector. Short dumps allowed us to monitor this noise. External noise sources were thus more easily identified and eliminated. However, the noise could not be completely eliminated. As a result, the detector was sent out for warranty repair. During this time, from August of 1993 to the beginning of December of 1993, a loaner from EG&G Ortec, a low-background POP-TOP detector with an efficiency of 48.5% was used. In addition during this period due to power supply problems, the PMT's of the round annulus were fried. It was replaced by the square annulus inside the Pb shield. Due to a mismatch in the gains of the PMT's of the two annuli, during that period Compton suppression was not used.

The only problem detected by Ortec on our GMX detector was spiking on the HV filter which was corrected. A comparison of the backgrounds with the square annulus and no Compton suppression and the round annulus and Compton suppression which is relevant for this series of experiments is given in **Figure 2-3**. Neither excess heat nor gamma ray activity above background were observed during the G cell on-line series runs. Thus, a meaningful correlation between excess power and a nuclear signature could not be established.

## Sample Counting 2

From December 3, 1993 to the beginning of last, fourth, G cell run, our detector was reintegrated into the system and the Compton suppression was brought up. Considerable effort was invested to reduce the electronics noise and eliminate the effects of ground loops. As a result the background was brought down to less than 2 c/s in the range of 10 keV to 2.5 MeV.

During this time a set of cathodes that was run in experiments aimed at producing simultaneous heat and He-4 by Bush were also counted. This group consisted of four electrodes. One was a 4 mm D x 8 mm long SmCePd electrode with rounded ends that originated in the Pons and Fleischmann laboratory and yielded a slight excess of power and a non-zero He-4 analysis result. The second was a Lot 2 Engelhard 2 mm x 2 cm cathode that gave a slight excess of power but no He-4. No. 3 was a Lot 3 Engelhard 2 cm x 2 mm with hemispherical ends that was heat treated and also gave a small amount of excess power and a non-zero He-4 analysis result. The last electrode of those counted was a 2 cm x 0.3 cm Engelhard Lot 3 vacuum melted that gave excess power as well. All the power excesses were on the order of 30 +/- 10 mW or a few percent of the input power. The He-4 measurements yielded numbers of a few parts per billion by volume but well above the background. No activity above background was observed.

## Sample Counting 3

At the end of the G4 run, a decision was made to abandon the "G" design partly due to the difficulties experienced in obtaining high loading in the G cell and partly due to the problems of forced liquid convective cooling. A series of Seebeck heat flow calorimeters was conceived. In the interim, the detector system, now considered reasonably noise free, was used to count our old electrodes. These can be divided into two groups: DOL electrodes and electrodes from calorimetric runs. Throughout, L cell cathodes were counted as experiments ended.

## Air Cooled Seebeck Calorimetry

In March 1994 a new strategy was developed to increase the likelihood of observing excess power in a cell monitored by the Ge detector. The strategy involved three sequential steps:

- a. Selecting a cell from a set of Degree of Loading (DoL) cells using high cathode loading as the criterion of selection.
- b. Transferring the selected DoL cell to a calorimeter designed to accommodate the whole cell, with minimal change or interruption.
- c. With the suggestion or indication of excess power, transfer the cell/calorimeter combination into the Ge detector.

A calorimeter was designed to accommodate a DoL quartz cell. Calorimetric measurements were made using the Seebeck effect to convert heat flow to a voltage. Eight Seebeck Thermo-Electric Devices (TED's) were placed, two per side, on the outside of a square Aluminum block, drilled to accommodate the cylindrical bottom section of a DoL cell. This configuration was cooled using electronic component cooling fins, acting as heat sinks, attached to the outer sides of the TED's. The cell top was reserved for electrochemical access, whereas the bottom affords the least obstructed line-of-sight for the Ge detector.

The Seebeck heat flow calorimeter was calibrated using, alternately and simultaneously, electrical and electrochemical heat sources in a calorimetrically open cell. On March 30, 1994, a cell was selected from the DoL K-series (designated as cell K1), and transferred to the Seebeck calorimeter for bench testing. This cell contained a 3 mm x 3 cm Engelhard Lot 2 Pd cathode, a helical Pt anode and 1.M LiOD with no additive. Inside the calorimeter, the cathode and cell were subjected to a series of current steps, ramps and brief anodic strips, in an attempt to regain the high loading levels previously demonstrated in the DoL "farm". A secondary purpose was to check the calorimeter calibration, observe the influence of passive and active air cooling on cell temperature and calorimeter function, and to search for indications of excess power.

The calorimeter, A-1, was operated in an enclosed "mini"-cubicle, on top of an electronic balance for a period of ~650 hours. Since the cell was operated in the open mode (no recombination catalyst - freely venting electrolysis gases), the purpose of the balance was twofold: 1) to ensure that the electrolyte level in the cell was maintained constant by a computer-controlled HPLC pump; 2) to measure the extent of recombination (if detectable) and assess the calorimetric implications of this phenomenon (if any). During this period of bench operation, the following observations were made in two extended current ramp/step sequences:

- i. The maximum loading achieved during the first ramp was  $D/Pd = 0.91$  at 148 hours following current (re)-initiation, at a current density of  $\sim 250$  mA cm<sup>-2</sup>.
- ii. The maximum excess power observed on the first ramp was  $40 \pm 30$  mW at 180 hours and a current density of 340 mA cm<sup>-2</sup>.
- iii. The calorimeter appeared well calibrated over the range of input powers (0-9 W) and currents (0-2A) examined [however, see point iv].

- iv. At higher temperatures, corresponding to high input power and low cooling rates, it is necessary to take into account the variation with temperature of the Seebeck coefficient in order to operate the calorimeter with a precision approaching 1%, or better.
- v. Rapid variations in the temperature difference between the cell and the heat sinks result in sometimes large transient heat flow across the TED's; the resulting voltage may obscure the slower response of the effect we are attempting to observe. Such transient temperature gradients may be produced by rapid changes in room temperature (normally maintained constant (within  $\pm 1^\circ\text{C}$ ), changes in cooling rate (forced air flow), and changes in input power (associated with current steps).
- vi. The transient calorimetric consequences of changes in temperature differential can be corrected for if the heat capacity of the cell and its contents, and the thermal time constant of the system is known. The heat capacity (water equivalent) was determined to be the equivalent of  $\sim 65$  g of water (depending somewhat on electrolyte level), and the calorimeter time constant  $t \approx 300$  s (5 minutes).
- vii. The influence of electrolyte level on the steady state calorimeter response was found to be negligible over the desirable and intended range of variation ( $\pm 1$  cm).
- viii. When operating at modest and high currents, Faraday's law appreciably underestimates the makeup heavy water requirement. It is probable that the additional D2O loss is via gas phase vapor transport of D2O-saturated electrolysis gases. This effect was observed to be a somewhat complex function of cell temperature and current. While this process is endothermic, and will thus tend to contribute to an under-estimate of  $P_{\text{xs}}$ , its calorimetric and electrochemical consequences can be severe. The D2O requirement cannot be calculated accurately from the Coulombs passed. Cells which do not have a reliable means of automatically determining electrolyte level, appropriately coupled to a reliable means of delivering needed D2O, may be either under- or over-watered. The electrochemical consequences of both are undesirable.
- ix. When operating a calorimeter open, one presumes that the electrolysis reaction yielding gaseous deuterium and gaseous oxygen is the only electrochemical reaction occurring, and that this reaction proceeds only to the right. Under these constraints, the power deposited by the electrochemical process is  $I(V-V_{\text{TN}})$ , where  $V_{\text{TN}}$  accounts for the energy content of the escaping electrolysis gases.

Three important phenomena may violate the above assumptions, reduce the effective  $V_{\text{TN}}$ , and give the appearance of excess power: 1) soluble impurities may be reversibly reduced and oxidized on the cathode and anode in an electrochemical shuttle; 2) molecular D<sub>2</sub> (or O<sub>2</sub>) dissolved in the electrolyte may be oxidized (or reduced) on the counter electrode; 3) molecular D<sub>2</sub> and O<sub>2</sub> may recombine in the gas phase (but still within the calorimeter), particularly on catalytic surfaces.

For the Al cell, a careful examination of the gravimetric consumption of D2O at low currents indicated that none of these three processes, electrochemical shuttle, subsurface re-reaction or gaseous recombination, were detectable.

A second current ramp was started on April 15, 1994, ~384 hours after current re-initiation. During this ramp the cell was observed to achieve a D/Pd loading of 0.94 at a current density of ~100 mA cm<sup>-2</sup> (4/16/94). At somewhat reduced loading (D/Pd ≥ 0.90), at current densities ≥ 275 mA cm<sup>-2</sup>, this cathode also exhibited a small amount of excess power, reaching a maximum of ~350 ± 30 mW, at a current density of 725 mA cm<sup>-2</sup>, on April 23, 1994. This excess power terminated with reduction in cathodic current density on April 26, 1994. The total integrated excess energy observed in this thermal excursion was 178 kJ or 7.4 MJ/Mole Pd.

Based on these observations and the possible indication of excess power during the second current ramp, the A1 cell and calorimeter were installed inside the NaI annulus, and on top of the Ge detector. As of May 12, 1994 and through July 8, 1994 the air cooled Seebeck heat flow calorimeter was operated in the environment of the gamma counter. Electrochemical current was re-initiated on 4/13/94 at 16:45.

Greater ease of operation was achieved with air cooling through a collar located under the table, on which was mounted the Pb passive shield, and at the opening for detector insertion into the shield. However, this advantage was somewhat offset by the fact that at higher air flow rates vibration became a problem. This manifested itself as a deterioration of the FWHM and a loss of the bottom end of the spectrum due to microphonic effects. Also of note is that even though the cooling fins are aluminum, the TED's themselves are made of semiconducting material and result in considerable gamma ray absorption.

In this configuration, the middle of the cathode is 7-cm above the detector. Coincidence peaks and all sum structures are less prominent in this spectrum than in the calibration spectra at the window of the detector.

On May 16, 1994 a series of current steps and ramps were initiated to confirm the calorimeter calibration and to attempt to re-load the cathode after the period of current interruption. On May 23, 1994 a loss of electrolyte event occurred due to high current and high temperature operation, in which the cathode was wholly, or largely, exposed to stoichiometric gas, instead of electrolyte. Analysis of the gamma spectra obtained leading up to, and immediately following the loss of electrolyte revealed no activity above background.

### **Possible Ag-111 Identification During the A1 Run**

Subsequent to the loss of electrolyte due to evaporation at higher temperatures, the decision was made to swap the EG&G loaner with our extra low background GMX detector. Counting commenced on May 27, at 17:41 h but without Compton suppression due to a difference in the gains at the outputs preamplifiers of the two Ge detectors.

Our GMX detector had not been used in this configuration with a DOL cell in a Seebeck air cooled calorimeter prior to this. However, due to the fact that at the time we were observing a live experiment, no background was taken.

A visual inspection of the spectrum indicated a possible peak at 342 keV. This weak signal grew over time, reaching almost a 5 sigma value on June 1, 1994 during the dump started at 9:51 am. The appearance of this peak is seen in **Figure 3-1**. The net counts in the peak are over 3 sigma and it satisfies in terms of FWHM for a small peak. The other peaks present are background peaks. Using the methodology mentioned earlier for predicting the development dynamics of small peaks, with data taken in intervals of equal length, it was concluded that there was cause to monitor the development of this peak.

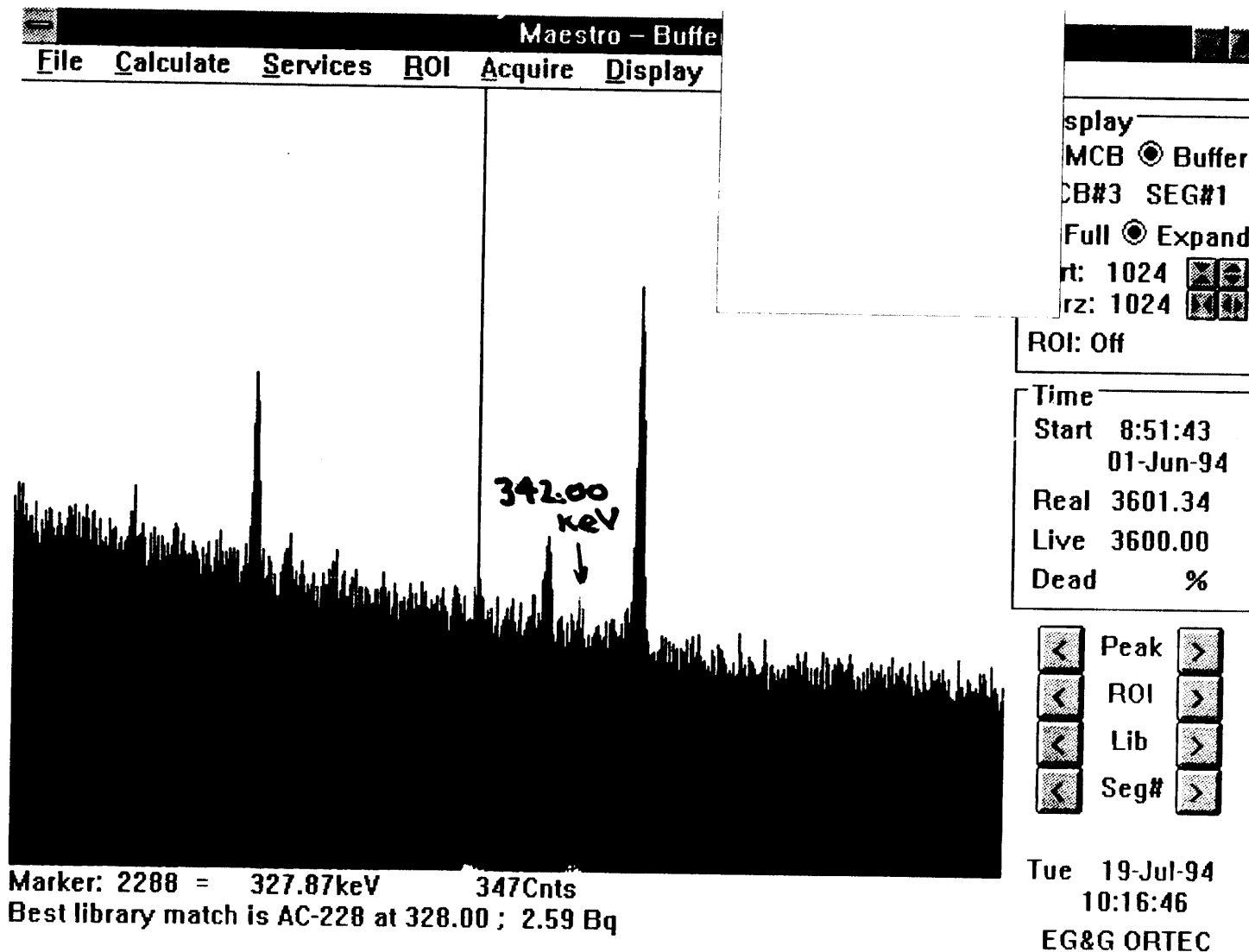


Figure 3-1  
Appearance of the 342 keV Gamma of Ag-111

The count balance in the ROI after 117 dumps of 1 hour or 421200 s reached 721 c +/- 185 or 4 sigma and was also identified by the Maestro II peak search routine at a sensitivity of 3. This corresponds to a count rate of  $1.64 \times 10^{-3}$  c/s +/-  $4.08 \times 10^{-4}$  c/s. The detector efficiency at 342 keV is ~5%. In addition, the geometry factor and material absorption are estimated to result in an efficiency of at least  $.6 \times 10^{-1}\%$ . Thus, with 6 gammas per 100 disintegrations, or  $((1.64 \times 10^{-3} \text{ c/s}) / (6 \times 10^{-3})) \times 16.67 = 4.55 \text{ d/s}$  (273 dis/min). Subsequently, this line sank into the background with a half-life of 8.5 days +/- 3.5 days due to the low statistics. This led us to search for a possible candidate.

Isotopes in the region around Pd were candidates. A possible candidate for this line is Ag-111. Ag-111 has two lines, the above at 342.1 keV at 6 gammas/100 disintegration's and a weaker line at 245.35 with 1 gamma/100 disintegrations. The half-life of this beta minus emitter is 7.45 days.

A possible production pathway for this isotope is Pd-110(d,n)Ag-111 and Ag-111m. This reaction has a positive Q of 4.97 +/- 0.5 MeV. However, the potential barrier is of the order of  $B_c = Zze^{*2}/R = Zz/A^{*}(1/3) = 5.36 \text{ MeV}$ . Pd110 has a 11.72% abundance. The Q's of the natural Pd isotopes are as follows:

**Table 3-1**  
**(d,n) reaction Q values for d on the natural Pd isotopes**

Natural Abundance	Reaction	Q Value
11.8%	Pd110 (d,n) Ag111	4.297 +/- 0.5 MeV
26.7%	Pd108 (d,n) Ag109	4.2023 MeV
27.3%	Pd106 (d,n) Ag107	3.33922 MeV
22.2%	Pd105 (d,n) Ag106	3.521 MeV
11.0%	Pd104 (d,n) Ag105	1.966 MeV
1.0%	Pd102 (d,n) Ag103	2.1603 MeV

The other possible channel through radioactive neutron capture on Pd-110(n,gamma)Pd-111 (beta emission)Ag-111 has a cross section of 6.9 barns. In our configuration, the thermalization probability is low and the absence of this channel is not unexpected. No Ag-111m or Pd-111 and Pd-111m lines were in evidence in the spectrum.

As a result of this observation, old spectra were inspected for the presence of this line. No lines at this energy of statistical significance were observed prior to this event. A background was also taken after this run. The 342 keV line was not observed. In addition, in view of the width of the observed line which is on the wide side for a line of such low statistics, the possibility of it being a doublet was entertained. The Maestro II smooth routine resulted in a peaked structure with two reasonably symmetric wings. This prompted us to send for a detailed FFT noise reduction analysis.

The result of this analysis indicated a doublet. The lines may be seen in **Figure 3-2**. No other lines were observed.

In an attempt to interpret these results a sample was neutron irradiated to check the half-life given in the tables. In addition this was a good test of the energy of the line. A sample was from the same lot was irradiated in a flux of  $2.82 \times 10^5$  n/cm<sup>2</sup> for one week in a well thermalized neutron flux. A comparison of just the lines with the background subtracted out in the calorimeter run and the irradiated sample confirms that the line is in the right position and that indeed it may be a doublet. In view of the low counting statistics for this gamma ray it is evident that further confirmation of the existence of this line is warranted.

### **Gamma Counting**

Following the May 23 rd loss of electrolyte during the first ramp performed inside the Ge detector, the A1 cell was again refilled with D2O and attempts were made to re-load the cathode with deuterium and to observe excess power again, this time in the vicinity of the Ge detector. These efforts were only partially successful.

A second ramp was attempted on June 2, 1994. The D/Pd loading reached a maximum of 0.90 at ~300 mA cm<sup>-2</sup>. This was accompanied by a possible indication of excess power, with a maximum Pxs ~70 ± 30 mW occurring on June 5, 1994 at an electrical input power of 8W. A third ramp in the Ge detector was started on June 23, 1994, and again give the superficial appearance of positive excess power with a maximum Pxs <sup>a</sup> 70 ± 30 mW. These observations of excess power during ramps 2 and 3 must, however, be treated with special caution for a number of reasons:

- i. The effect observed was very small, less than 1% of the electrochemical input power. While this percentage is larger than the measurement precision and calibration accuracy outside the Ge detector, no calibration had been performed in the constrained geometry of the detector.
- ii. The excess power observed for both ramps was the same, in each case closely paralleling the electrochemical input power. This suggests a systematic or calibration error.
- iii. Because of the confined geometry within the Ge detector and problems induced in the detector by microphonic effects, the flow of air cooling to the calorimeter was substantially less in the detector than outside. As a consequence, the cell operated at much higher temperatures inside the detector than outside, and the TED's were operated outside their calibration range. It is suggested, therefore, that the ~1% excess power apparently observed during ramps 2 and 3 inside the Ge detector, was due to miscalibration of the TED's and calorimeter. The gamma spectra were nevertheless analyzed in the intervals 6/2/94 - 6/18/94 and 6/24/94 - 7/3/94, corresponding to the time of the two ramps.

Though great attention was paid to the possible recurrence of the Ag111 line, the gamma spectra taken during this period did not differ from background. The Ag-111 line was not seen again nor did any new lines appear.

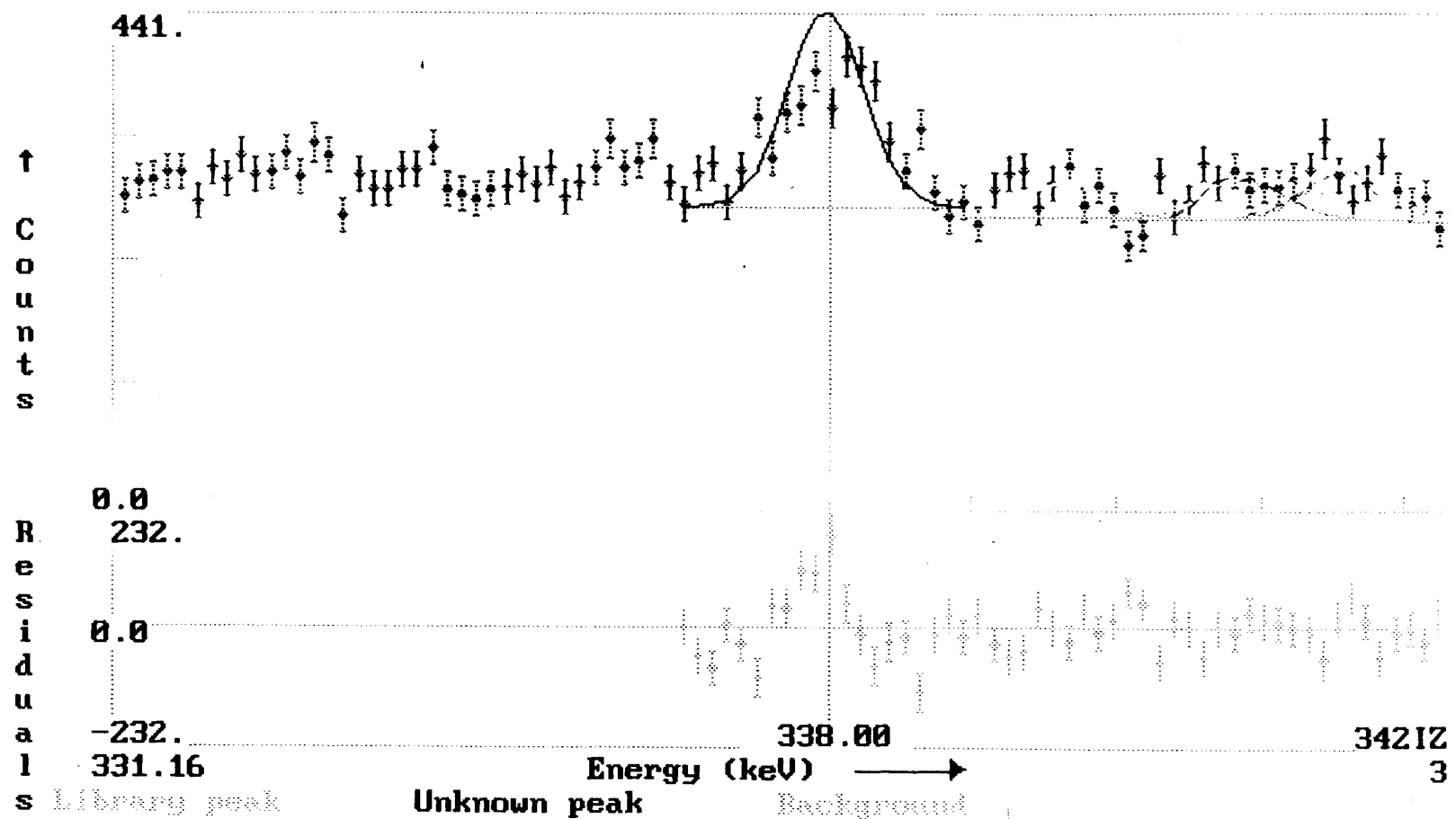


Figure 3-2  
Appearance of the Doublet Nature of the Ag-111 Peak

Another problem was manifest in the A1 cell while operating inside the Ge detector. No visible means of inspection or level sensor with reliable feedback was provided for the cell. When removed from the electronic balance and placed on the Ge detector, it became very difficult to define and maintain the cell electrolyte level. Towards the end of the A1 experiment, on July 1, 1994, the current was stepped from 0.425 to 2.0 A in an attempt to explore the effects of temperature and deuterium flux on gamma emission and/or excess heat production. At this point the cathode resistance ratio measured 1.5. This either indicates a very high loading,  $D/Pd \approx 1.0$  on the right side of the resistance maximum, or a very low loading,  $D/Pd \approx 0.4$  on the left hand side of the resistance maximum. Both values are implausible for the average loading of a Pd cathode under normal electrolysis conditions. Approximately two hours after the current step, the apparent excess power was observed to increase from  $0 \pm 50$  mW to  $\sim 3$  W. This excess power persisted for nearly 12 hours at constant input power, causing the cell temperature to rise to nearly  $80^\circ\text{C}$ . Thus the heat source was real and substantial. The output power was in excess of the input power assuming that the cell was thermodynamically open;  $P_{in} = I \cdot (V - V_{TN})$ . However, the output power was equal to the input power for a thermodynamically closed cell;  $P_{in} = I \cdot V$ .

These two anomalies, the unusually low resistance ratio and the appearance of unexpected excess power, can both be explained if the electrolyte level was sufficiently low to expose a large fraction of the cathode length. Only that portion of the cathode below the electrolyte level and exposed to the electrochemical process, can attain a loading greater than the 1 Atmosphere equilibrium value ( $D/Pd \approx 0.7$ ,  $R/R^\circ \approx 2$ ). The portion of the cathode that is exposed, must have a lower loading and resistance ratio. Furthermore, the exposed cathode may act as a site for combination and recombination of  $D_2$  and  $O_2$  so that the cell is thermodynamically closed.

The problem of ensuring constant, precise, and completely reliable electrolyte level control in cells that cannot be monitored visually or gravimetrically, remains to be solved.

Throughout the remainder of the AG cell runs no activity above background was detected.

## **Stand-alone NaI(Tl) detection System**

### ***NaI(Tl) Detector***

NaI(Tl) detectors are the most efficient detectors of gamma radiation. Their drawbacks are a high FWHM making identification less reliable and a high lower end energy around 70-80 keV due to encapsulation to protect against moisture.

However, these detectors, being easy to use and portable are a first choice for monitoring bulky systems and systems to which access is limited.

The NaI plug and the square annulus were instrumented for just such experiments, the main problem being the high background of such detectors. The plug has been and will be used to monitor whole baths. The square annulus will be used for monitoring batteries of experiments position around it. In this case, when signals are taken of the PMT's individually, we have a measure of position resolution. This also applies to height.

## **Electronics, Data Acquisition and Handling**

The electronics used to run the NaI(Tl) detectors are:

1. EG&G Ortec 113 PMT preamplifier
2. Microace 1K PC supported MCA card
  
- 3-1. Wolf, K., Shoemaker, J., Coe, D., and Whitesell, L., “Neutron Emission from Deuterium-Loaded Metals”, Proceedings of the Conference on Anomalous Nuclear Effects in Deuterium/Solid Systems, AIP Conference Proceedings 228, Provo, Ut. 1990.



# 4

## FAST NEUTRON SPECTROMETER

---

### Detection System

#### ***Dual NE-213 Neutron Detectors***

Two liquid scintillator BC 501A 5" x 3" coupled to PMT's make up the detector part of our fast neutron spectrometer. These detectors have good time resolution and high signal to noise ratios. Their resolution is however low, making them a spectrometer in the limited sense. However, they can satisfactorily differentiate 1 MeV, 2.5 MeV and 14 MeV neutrons.

These detectors are sensitive to both gamma rays and neutrons via the electronic and proton recoil signals. Due to the different time behavior of these signals, the gamma signals can be gated out using pulse shape discrimination.

#### ***Active Cosmic Ray Suppression***

Though PSD allows us to gate out a considerable fraction of the gamma ray background, about 10% of the overall count rate will nevertheless seep through. In order to diminish this fraction of the gamma ray background, active gamma ray shields are used. These shields in effect also halve the neutron background because CR neutrons are entrained in gamma ray showers.

Six 60 cm x 40 cm plastic scintillator shields made of BC416 1/4" thick coupled to photomultiplier tubes are used to generate a signal that is then used to veto the neutron counter system.

#### ***Passive Shielding (Thermalization)***

Passive shielding in the form of hydrogenous material is used to protect the experiment from external neutron sources by way of thermalizing them out of the range of detection.

#### ***NIM-CAMAC Electronics and Power Supplies***

The electronics for the neutron station are a CAMAC-NIM hybrid, all the modules except the independent gate charge sensitive ADC are NIM. The ADC is supported by a Kinetic Systems CAMAC crate and crate controller. The signal is passed through a Canberra 2160A. Pulse Shape Discriminator and processed until it is fed to the Le Croy model 2249A 12 channel ADC. The signal from the CR paddles gates this ADC.

## **Data Acquisition and Software**

An Apple computer is used for data acquisition. MAC supported K - Max software allows for event by event data taking and spectrum acquisition.

# 5

## CONCLUSIONS

---

The primary goal of the nuclear effort at SRI is to search for the nuclear signature of cold fusion. This incorporates the establishment of a correlation between excess heat and a nuclear signature. In the absence of nuclear events, upper limits to the nuclear radiation vs. excess heat relationship were attempted to be established.

During the period of this contract, a major and excellent nuclear detection facility was built and instrumented. The systems were designed to monitor calorimeters while they were producing excess heat. During this time, however, though they occurred elsewhere in the laboratory, no excess heat events occurred while under surveillance in the nuclear detection systems. This precluded the search for the correlation between excess heat and its nuclear signature. The only possible nuclear event occurred at a time of no excess heat. Furthermore, the search for activation on old cathodes did not yield a positive result.

Thus, the correlation of excess heat and a nuclear signature awaits the reliable reproduction of excess heat of sufficient magnitude to justify and warrant a nuclear source.

The reports of substantial gamma ray activity from other laboratories and our own possible identification of Ag-111, however, prompt us to consider how to best reproduce these results either within the effort to establish a correlation with excess heat or as a separate effort.

It is curious that the event apparently triggering the appearance of the 342 keV gamma ray of Ag-111 was a loss of electrolyte in which the highly loaded palladium cathode was exposed to the vapor phase of the cell. This event results in rapid deloading of the exposed part of the cathode accompanied by a rise in temperature from recombination of electrolysis gases at the cathode surface. This transient may be related to the transient to which Wolf exposed his cell cathodes from a cryogenic episode followed by gradual warmup. Wolf apparently observed a number of nuclear reactions interpretable as deuteron and proton reactions with each of the stable palladium isotopes - reactions previously seen only with high energy accelerated deuterons and protons.



# 6

## GLOSSARY AND DEFINITION OF ACRONYMS

---

**HPGe** - High purity germanium, often called intrinsic germanium.

**Efficiency** - is a measure of how many pulses occur for a given number of gamma rays.

- a. Absolute efficiency - The ratio of the number of counts produced by the detector to the number of gamma rays emitted by the source in all directions.
- b. Intrinsic efficiency - The ratio of the number of pulses produced by the detector to the number of gamma rays striking the detector.
- c. Relative efficiency - The efficiency of the germanium detector relative to a 3 in. diameter 3 in. long NaI crystal each at 25 cm from a point source at 1.33 MeV.
- d. Full-Energy (Photopeak) Efficiency - The efficiency for producing full-energy peak pulses only.

**POP-TOP** - EG&G brand name for transplantable detector capsules.

**GMX** - EG&G brand name for a thin-window coaxial detector used from 3 keV to 10 MeV.

**FWHM** - Full Width at Half Maximum.

The full width of an energy peak measured at one-half of its maximum amplitude with the continuum removed. It defines the resolution of a spectroscopy system, e.g. the ability of a system to differentiate or resolve two close peaks.

**Resolution** - The energy resolution **R** of a detector is defined as the FWHM divided by the location of peak centroid.

**ROI** - Region of interest is a user defined area of the histogram which contains data of interest.

**Peak area** - The data displayed by Maestro II are net area, gross area and the error of the net area for the ROI peak that is marked. The background on the low channel side of the peak is the average of the first three channels of the ROI. The channel number for this background point is the middle channel of the three points. The same applies for the background on the high side. These two points on each side of the peak form the end points of the straight line background. The background is given by the following:

where

B - background area

l - the ROI low limit

h - the ROI high limit

C<sub>i</sub> - the contents of channel i

6 - the number of data channels used (3 at each end)

The gross area is the sum of all channels marked by the ROI according to the following:  
A<sub>g</sub> - where

A<sub>g</sub> - the gross counts in the ROI

l, h and C<sub>i</sub> - as above.

The adjusted gross area is the sum of all the channels marked by the ROI but not used in the background according to the following:  
A<sub>ag</sub> = where

A<sub>ag</sub> - adjusted gross counts in the ROI and the rest of the nomenclature as above. The net area is the adjusted gross area minus the adjusted calculated background

A<sub>n</sub> = A<sub>ag</sub> -

The error in the net area is the square root of the sum of the squares of the errors in the adjusted gross area and the weighted error of the adjusted background. The background error is weighted by the ratio of the adjusted peak width to the number of channels used to calculate the adjusted background.

**CS** - Compton suppression

**Peak-to-Compton** - A measure of the fraction of gamma quanta absorbed by the detector and defined as the ratio of the mean number of counts in a region of the Compton continuum (away from the Compton edge) and the number of counts in the peak channel. For a Cs-137 source the Compton continuum region is between 358 and 382 keV and the relevant number is the total number of counts in this region divided by the number of channels into which it falls.

**NIM** - Nuclear Instrumentation Module standard.

**PC** - IBM or clone personal computer

**MCA** - Multichannel analyzer

**PMT** - Photomultiplier tube

**HV** - high voltage

**ADC** - Analog to digital converter

**TAC/SCA** - Time-to-amplitude converter/single channel analyzer combination

**FFA-CFD** - Fast filter amplifier - Constant fraction discriminator combination

**CAMAC** - Computer Automated Measurement and Control Standard

**DoL** - Degree of Loading Cell

**TED** - Thermoelectric device, refers to Seebeck heat flow calorimeter elements

**CAMAC** - Computer Automated Measurement and Control Standard

**PSD** - Pulse shape discrimination

**CR** - cosmic ray



# **A**

## **APPENDIX A: SUMMARY OF THE OBSERVATIONS AT TEXAS A&M BY KEVIN WOLF**

---



**EPRI/NPD**

**SIGNIFICANCE OF TEXAS A& M  
FINDINGS IN OCT. 1992**

**THOMAS O. PASSELL**

**August 5, 1993**

**August 1993**

**EPRI/NPD**

## **THE FINDINGS BY KEVIN WOLF**

- 3 Cells Electrolyzed in Series at Constant Current 6 weeks near a Neutron Detector of Low Background (40 Counts/Hr) using a New Protocol of Adding Boron and Aluminum at 0.001 Molar to the 0.1 Molar LiOD Electrolyte at the 18th Day
- Cathodes Were Loaded With Deuterium Slowly at a Few 10's of milliamps/cm<sup>2</sup> With a Cryogenic 12-Hour Treatment @ 17 Day Point and Were Sanded Every 7 Days and Replaced in the Cells within a 15 Minute Period Each Time
- On the ~21st & 22nd Days Two Successive Neutron Episodes Were Observed at About 2 to 3 Times the Background Rate. The Neutron Detector is Minimally Sensitive to Gamma Rays and Such Were Observed Near the End of the 20-Hour & 4-Hour Neutron Episodes
- Upon Dismantling the Cells the Cathodes (6 mm Diameter x 60 mm Long) Were Observed to be Mildly Radioactive.
- Analysis by High Resolution Germanium Gamma Detectors Revealed Presence of 10 to the 11th Atoms of Silver, Palladium, Rhodium, and Ruthenium Isotopes Having Ratios that Preclude Production by High Energy Deuterons

**August 1993**

**EPRI/NPD**

## **Tentative Conclusions if Wolf's Findings are Confirmed**

- Neutron Capture is Precluded as the Primary Mechanism Because Beta Decay Cannot Produce these Particular Isotopes by Neutrons on Palladium
- Deuterons or Protons Must Have Entered the Palladium Nuclei with the Subsequent Emission of Alpha (Helium-4) Particles and Possibly Particles of Higher Mass and Atomic Number
- Since the Protocol for Achieving this Phenomena was Similar to that Found at SRI for Producing Excess Heat, There May be Some Connection With Excess Heat Production
- Wolf's Cells Not Instrumented to Observe Excess Heat
- Since All 3 Cathodes Were Activated to Degrees Varying by no more than a Factor of 3 and Since 2 Neutron Episodes Were Noted, It should be Possible to Replicate the Events - Now Under Way - However the First Two Replication Attempts Have Failed to Show the Effect

**August 1993**

**EPRI/NPD**

**Wolf's Findings**

•Isotopes Seen in Most Active One of Three Cathodes ~9-7-92 at Texas A&M

•••ISOTOPE••• NO. of ATOMS RELATIVE NO.

•Silver-110m	0.8 Billion	1
•Rhodium-99	2.7 Billion	3.4
•Ruthenium-103	3.7 Billion	4.6
•Silver-106m	4.5 Billion	5.6
•Rhodium-102m	6.3 Billion	8
•Palladium-100	7.7 Billion	9.6
•Rhodium-102	12 Billion	15
•Rhodium-101	12 Billion	15
•Rhodium-101m	22 Billion	28
•Silver-105	26 Billion	32

Note: Atom Numbers are those present at the time of production ~ 9-7-92 (Total is 98 Billion)

**August 1993**

**EPRI/NPD**

## **Postulated Reactions to Produce The Observed Isotopes**

<b>PRODUCT</b>	<b>REACTION</b>
•Silver-110m	Pd-108 (d,Gamma) (Q=+10.9 Mev) or on Impurity Silver -Ag-109 (d,p) (Q=+4.5 Mev)
•Rhodium-99	Pd-102(p,Alpha) (Q=+3.2 Mev)
•Ruthenium-103	Pd-106(d,pAlpha) (Q=+1.2 Mev) or Ru-102(d,p)Ru-103 (Q=4.14 Mev) on Impurity Ru
•Silver-106m	Pd-105(d,n) (Q=+3.5 Mev) or Pd-105(p,gamma) (Q= +5.8 Mev)
•Rhodium-102	Pd-104(d,Alpha) (Q=+8.1 Mev) or Pd-105(p,alpha) Q= +3.6 Mev
•Rhodium-101	Pd-104(p,Alpha) (Q=+3.2 Mev)
•Silver-105	Pd-104(d,n) (Q=+2.0 Mev) or Pd-104(p, gamma) (Q= +4.2 Mev)

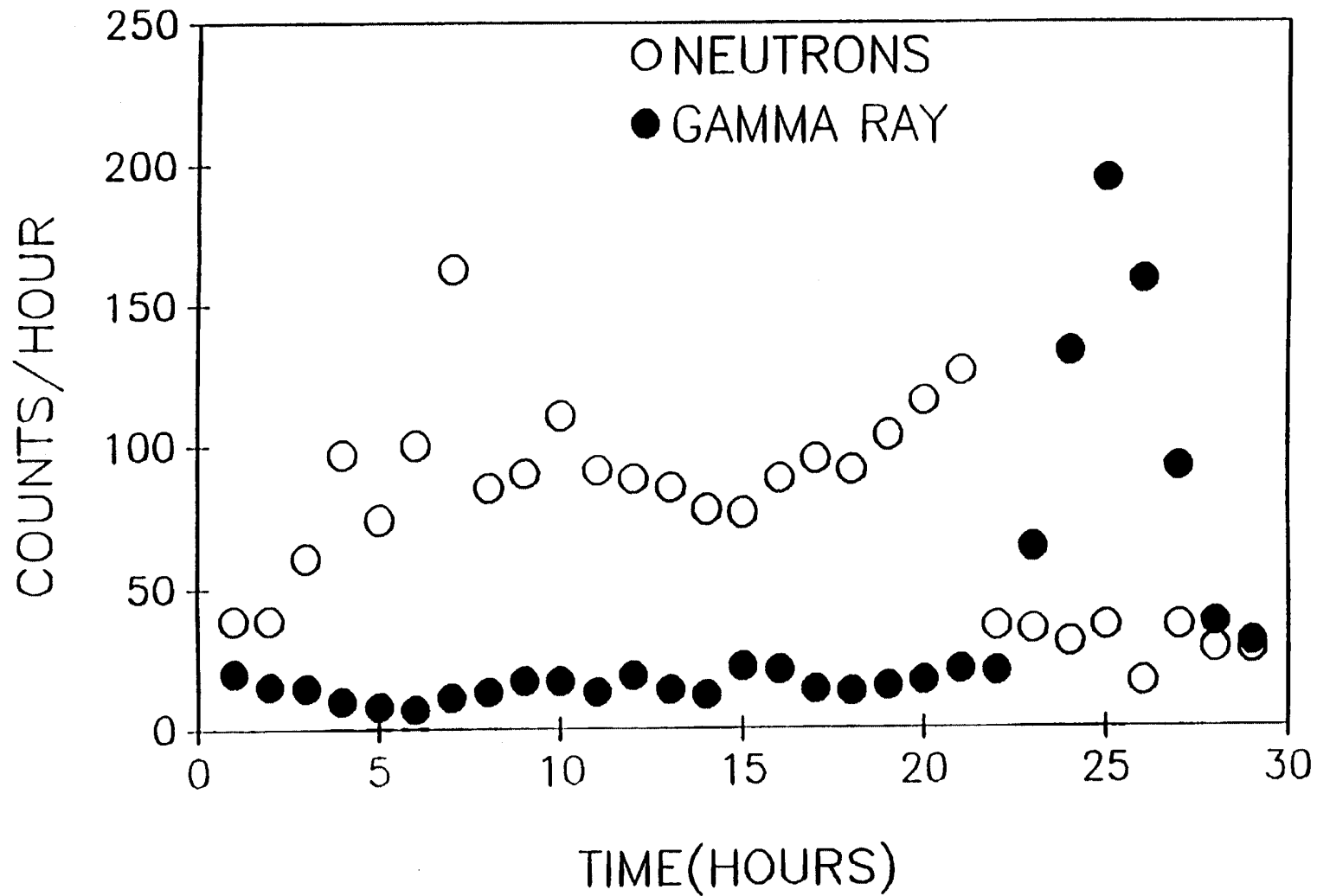
**August 1993**

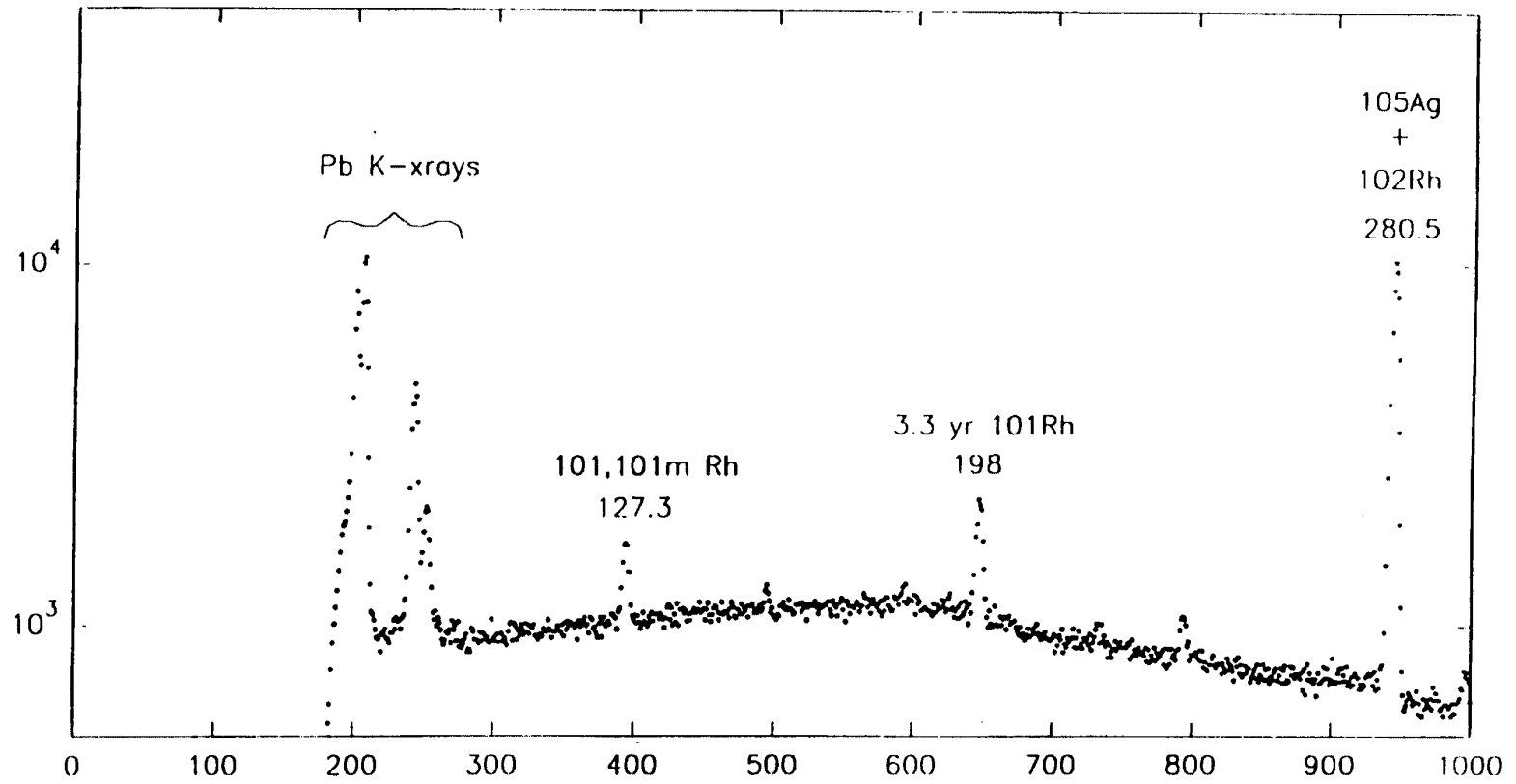
**EPRI/NPD**

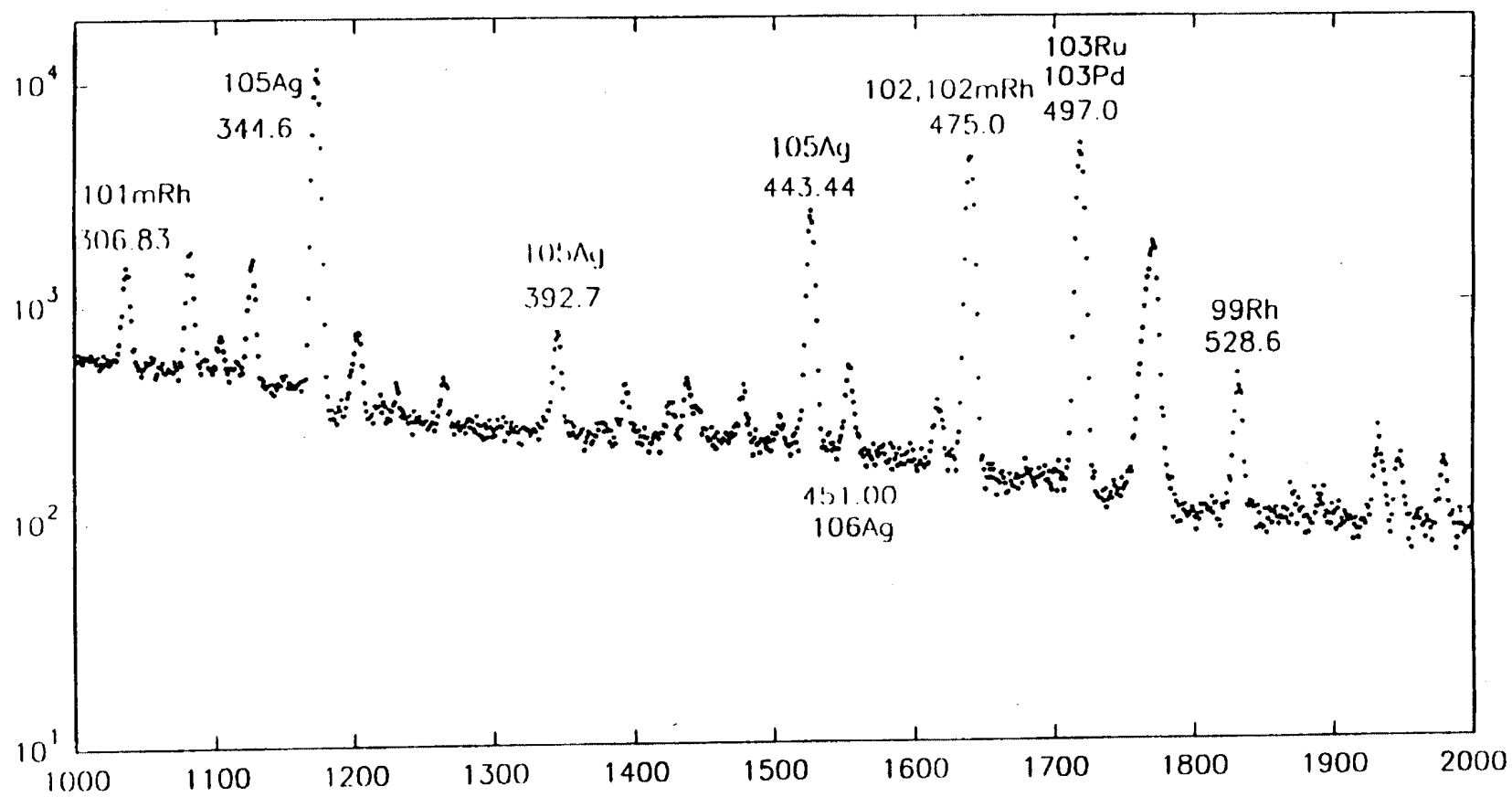
## **Tentative Conclusions if Wolf's Findings are Confirmed**

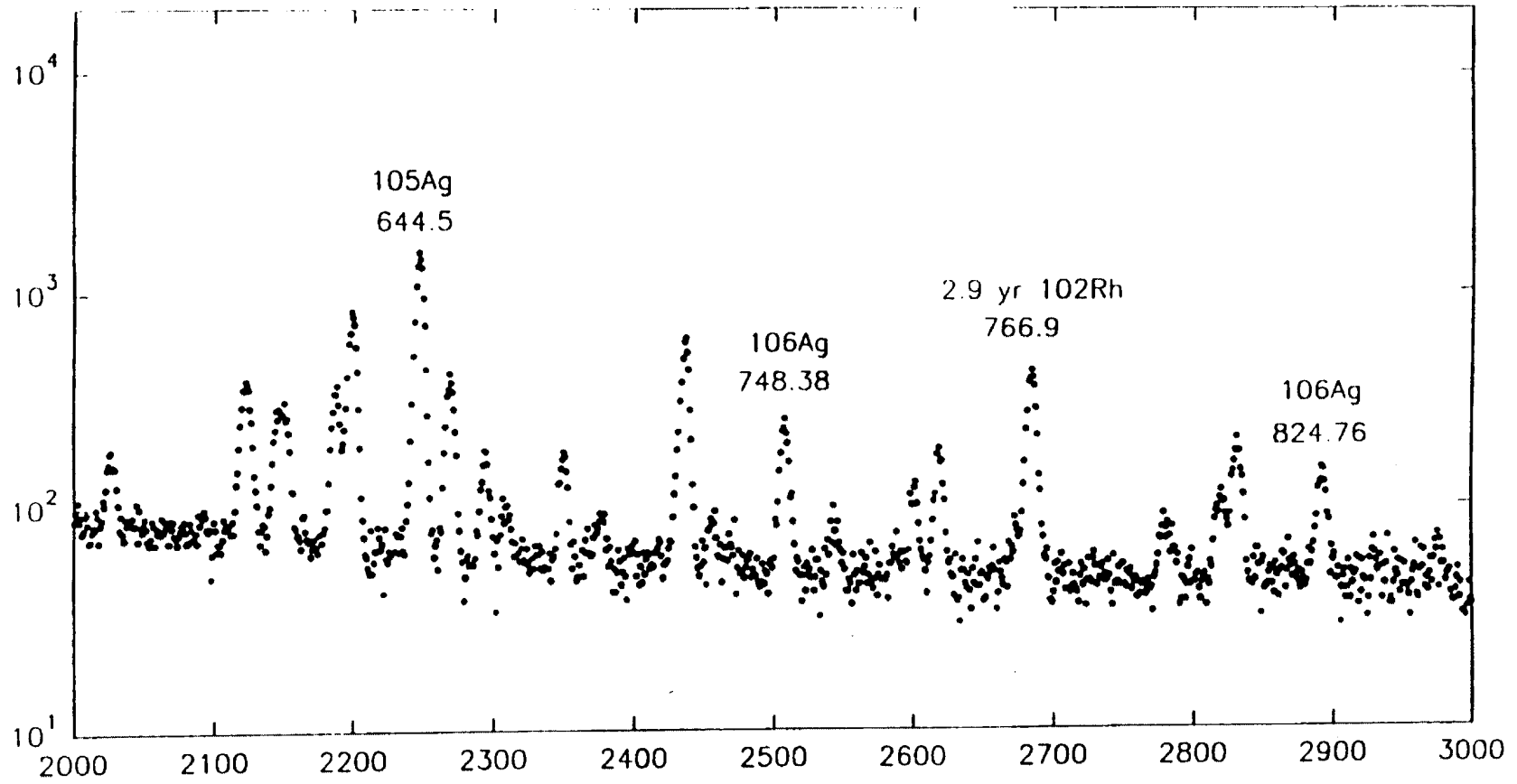
- If Deuterons Can Enter Palladium Nuclei, So also Should Protons (Light Water) Be Able To Under Similar Loading Conditions
- If Protons Can Enter a Nucleus of This High an Atomic Number (46), Then Maybe the Light Water Excess Heat Measurements Being Reported on Nickel (28), Silver (47), Tin (50) and Gold (79) Will Show Some Nuclear Signatures Also if We Look for Them.
- Also the Electrolyte Atoms that Diffuse into Cathodes May Be Similarly Activated By Deuterons or Protons to give Both Heat and Nuclear Reaction Products
- If the Palladium Reactions are Confirmed in D<sub>2</sub>O, then Other Nuclear Reactions Leading to Stable Nuclei in this Region of the Isotopes Chart Should be Produced - but not Easily Observed
- Since the Activation Levels in Pd are Many Orders of Magnitude Above Common Backgrounds, this Gives us a Nuclear Signature That is Unequivocal and Observable Outside the Cells Because of the Relatively High Penetrating Power of The Gamma Rays

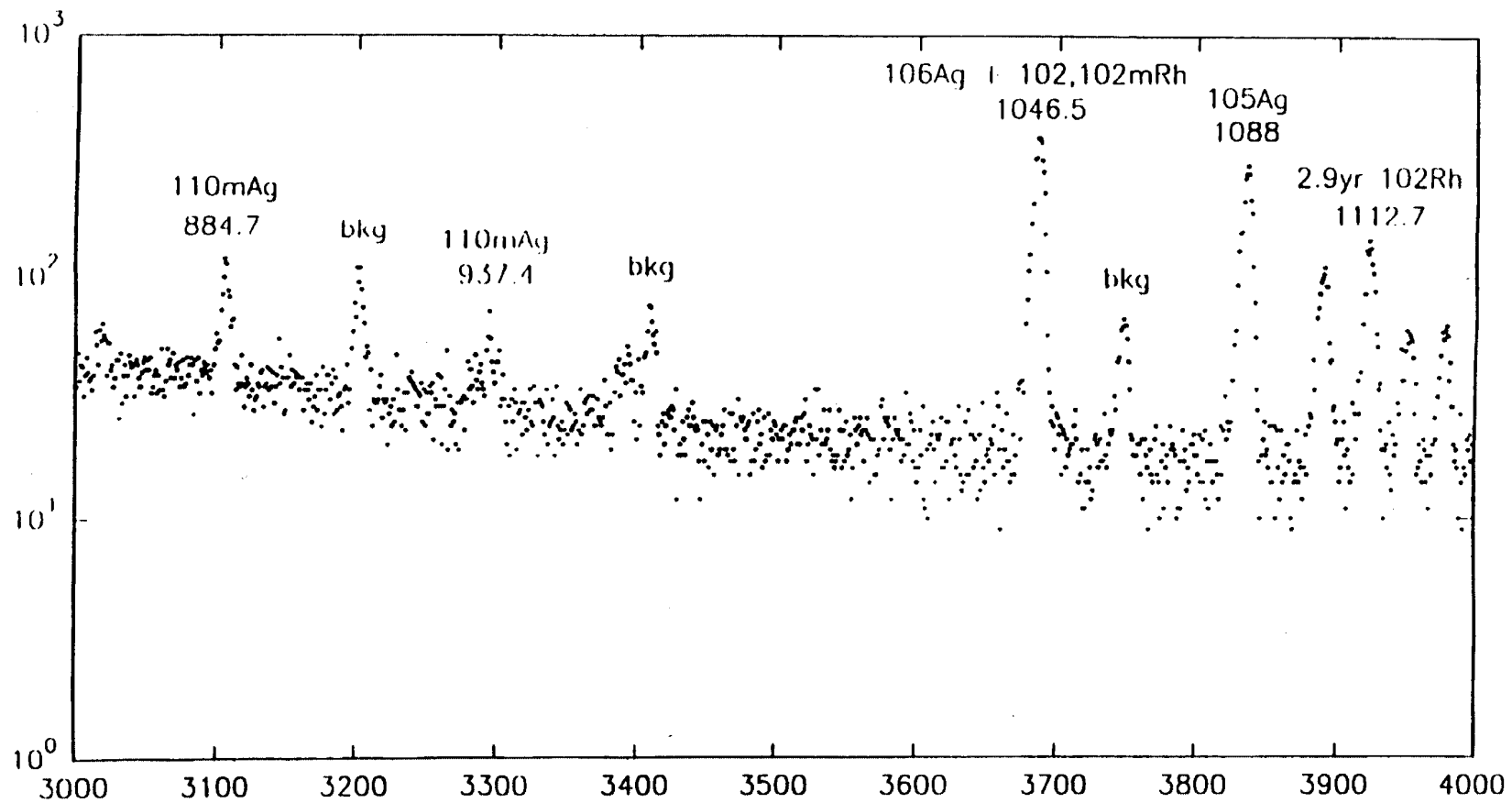
**August 1993**

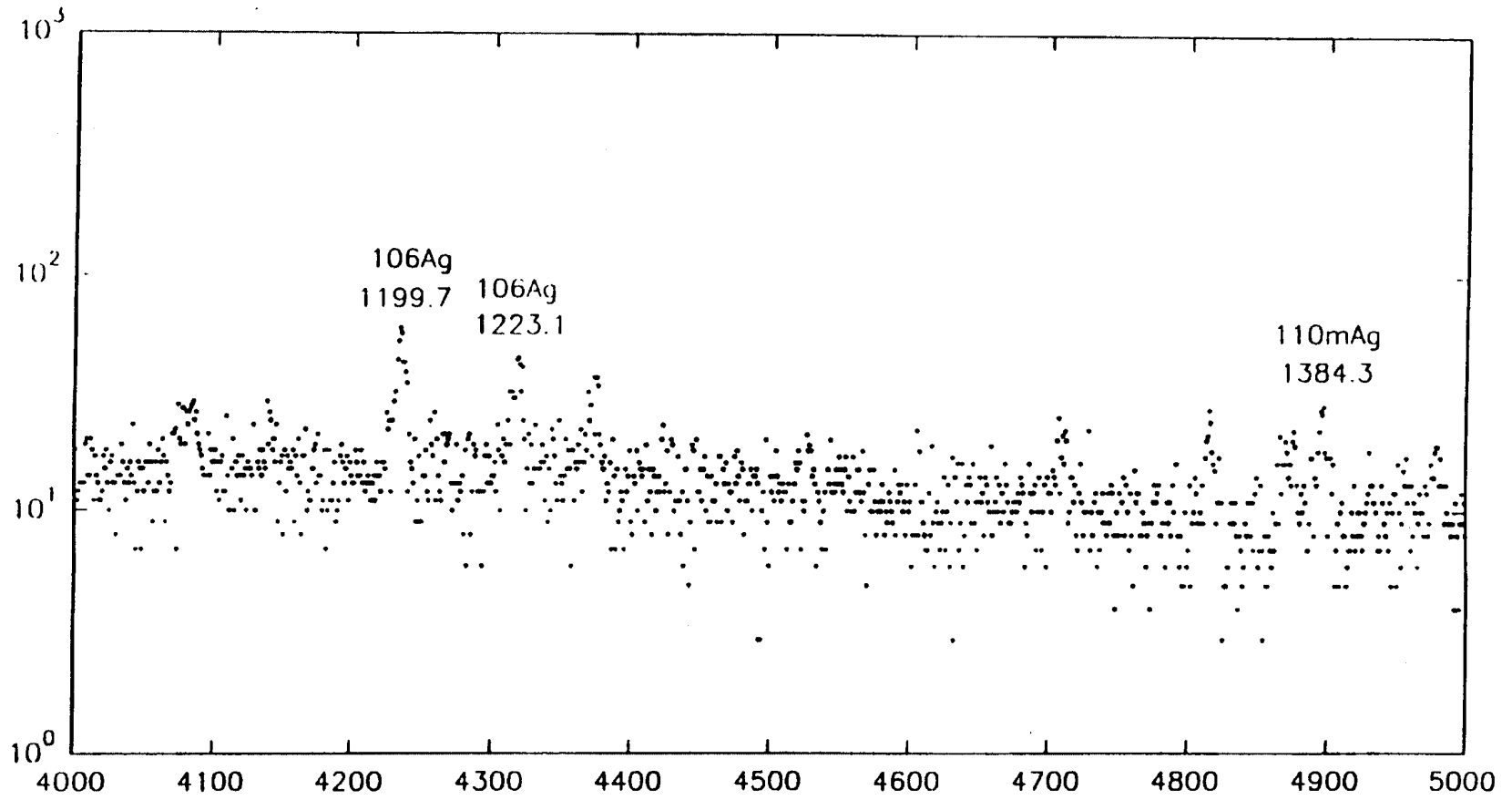
















**WARNING:** This Document contains information classified under U.S. Export Control regulations as restricted from export outside the United States. You are under an obligation to ensure that you have a legal right to obtain access to this information and to ensure that you obtain an export license prior to any re-export of this information. Special restrictions apply to access by anyone that is not a United States citizen or a Permanent United States resident. For further information regarding your obligations, please see the information contained below in the section titled "Export Control Restrictions."

### Export Control Restrictions

Access to and use of EPRI Intellectual Property is granted with the specific understanding and requirement that responsibility for ensuring full compliance with all applicable U.S. and foreign export laws and regulations is being undertaken by you and your company. This includes an obligation to ensure that any individual receiving access hereunder who is not a U.S. citizen or permanent U.S. resident is permitted access under applicable U.S. and foreign export laws and regulations. In the event you are uncertain whether you or your company may lawfully obtain access to this EPRI Intellectual Property, you acknowledge that it is your obligation to consult with your company's legal counsel to determine whether this access is lawful. Although EPRI may make available on a case by case basis an informal assessment of the applicable U.S. export classification for specific EPRI Intellectual Property, you and your company acknowledge that this assessment is solely for informational purposes and not for reliance purposes. You and your company acknowledge that it is still the obligation of you and your company to make your own assessment of the applicable U.S. export classification and ensure compliance accordingly. You and your company understand and acknowledge your obligations to make a prompt report to EPRI and the appropriate authorities regarding any access to or use of EPRI Intellectual Property hereunder that may be in violation of applicable U.S. or foreign export laws or regulations.

### About EPRI

EPRI creates science and technology solutions for the global energy and energy services industry. U.S. electric utilities established the Electric Power Research Institute in 1973 as a nonprofit research consortium for the benefit of utility members, their customers, and society. Now known simply as EPRI, the company provides a wide range of innovative products and services to more than 1000 energy-related organizations in 40 countries. EPRI's multidisciplinary team of scientists and engineers draws on a worldwide network of technical and business expertise to help solve today's toughest energy and environmental problems.

EPRI. Electrify the World

---

*Program:*

TR-107843-V2

Nuclear Power

---

© 1999 Electric Power Research Institute (EPRI), Inc. All rights reserved. Electric Power Research Institute and EPRI are registered service marks of the Electric Power Research Institute, Inc. EPRI. ELECTRIFY THE WORLD is a service mark of the Electric Power Research Institute, Inc.

Printed on recycled paper in the United States of America